Published Ahead of Print on July 19, 2018, as doi:10.3324/haematol.2018.193391.
Copyright 2018 Ferrata Storti Foundation.

EUROPEAN HEMATOLOGY ASSOCIATION

haematologica

Journal of the European Hematology Association
Owned & published by the Ferrata Storti Foundation

Inhibition of Btk by Btk-specific concentrations of ibrutinib and acalabrutinib delays but does not block platelet aggregation to GPVI

by Phillip L.R. Nicolson, Craig E. Hughes, Stephanie Watson, Sophie H. Nock, Alexander T. Hardy, Callum N. Watson, Samantha J. Montague, Jean-Daniel Malcor, Mark R. Thomas, Alice Y. Pollitt, Michael G. Tomlinson, Guy Pratt, and Steve P. Watson

Haematologica 2018 [Epub ahead of print]

Citation: Phillip L.R. Nicolson, Craig E. Hughes, Stephanie Watson, Sophie H. Nock, Alexander T. Hardy, Callum N. Watson, Samantha J. Montague, Jean-Daniel Malcor, Mark R. Thomas, Alice Y. Pollitt, Michael G. Tomlinson, Guy Pratt, and Steve P. Watson. Inhibition of Btk by Btk-specific concentrations of ibrutinib and acalabrutinib delays but does not block platelet aggregation to GPVI.
Haematologica. 2018; 103:xxx
doi:10.3324/haematol.2018.193391

Publisher's Disclaimer.
E-publishing ahead of print is increasingly important for the rapid dissemination of science.Haematologica is, therefore, E-publishing PDF files of an early version of manuscripts thathave completed a regular peer review and have been accepted for publication. E-publishingof this PDF file has been approved by the authors. After having E-published Ahead ofPrint, manuscripts will then undergo technical and English editing, typesetting, proof correction and be presented for the authors' final approval; the final version of the manuscriptwill then appear in print on a regular issue of the journal. All legal disclaimers thatapply to the journal also pertain to this production process.

Title Page

Inhibition of Btk by Btk-specific concentrations of ibrutinib and acalabrutinib delays but does not block platelet aggregation to GPVI

Short Title: Btk inhibitors on platelet activation

Phillip LR Nicolson[1], Craig E Hughes[2], Stephanie Watson[1], Sophie H Nock[2], Alexander T Hardy[1], Callum N Watson[1], Samantha J Montague[3], Jean-Daniel Malcor[4], Mark R Thomas[1], Alice Y Pollitt[2], Michael G Tomlinson[5], Guy Pratt[6], Steve P Watson[1,7]

[1]Institute of Cardiovascular Sciences, College of Medical and Dental Sciences, University of Birmingham, Edgbaston, Birmingham, B15 2TT, UK

[2]Institute for Cardiovascular and Metabolic Research, Harborne Building, University of Reading, Reading, RG6 6AS, UK

[3]ACRF Department of Cancer Biology and Therapeutics, John Curtin School of Medical Research, Australian National University, Canberra, ACT, 2601, Australia

[4]Department of Biochemistry, University of Cambridge, Downing Site, Cambridge CB2 1QW, UK

[5]Department of Biosciences, College of Life and Environmental Sciences, University of Birmingham, Edgbaston, Birmingham, B15 2TT, UK

[6]Department of Haematology, Queen Elizabeth Hospital, Birmingham, B15 2TH, UK

[7]Centre of Membrane Proteins and Receptors (COMPARE), Universities of Birmingham and Nottingham, Midlands, UK

Authors for correspondence:

Dr Phillip Nicolson, Institute of Cardiovascular Sciences, IBR Building, College of Medical and Dental Sciences, University of Birmingham, Birmingham B15 2TT; **e-mail:** p.nicolson@bham.ac.uk; **Tel:** 0121 415 8678

Prof Steve Watson, Institute of Cardiovascular Sciences, IBR Building, College of Medical and Dental Sciences, University of Birmingham, Birmingham B15 2TT; **e-mail:** s.p.watson@bham.ac.uk; **Tel:** 0121 414 6514

Text word count: 4543

Abstract word count: 179

Figures: 7

Tables: 0

Supplementary Figures: 3

Supplementary Tables: 2

No. of references: 42

Scientific Category: Platelets and Thrombopoiesis

Key points

- Btk blockade by ibrutinib and acalabrutinib delays but does not block platelet aggregation to maximal GPVI stimulation
- Clinical doses of Ibrutinib but not acalabrutinib block platelet aggregation to GPVI agonists due to off-target effects

Abstract

Ibrutinib and acalabrutinib are irreversible inhibitors of Bruton's tyrosine kinase used in the treatment of B cell malignancies. They bind irreversibly to cysteine 481 of Bruton's tyrosine kinase, blocking autophosphorylation on tyrosine 223 and phosphorylation of downstream substrates including phospholipase-□2. In the present study, we demonstrate that concentrations of ibrutinib and acalabrutinib that block Bruton's tyrosine kinase activity as shown by loss of phosphorylation at tyrosine 223 and phospholipase-□2 delay but do not block aggregation to a maximally-effective concentration of collagen related peptide or collagen. In contrast, 10-20 fold higher concentrations of ibrutinib or acalabrutinib block platelet aggregation to Glycoprotein VI agonists. *Ex vivo* studies on patients treated with ibrutinib, but not acalabrutinib, show a reduction of platelet aggregation to collagen related peptide indicating that the clinical dose of ibrutinib but not acalabrutinib is supramaximal for Bruton's tyrosine kinase blockade. Unexpectedly, low concentrations of ibrutinib inhibit aggregation to collagen related peptide in patients deficient in Bruton's tyrosine kinase. The increased bleeding seen with ibrutinib over acalabrutinib is due to off-target actions of ibrutinib that occur because of unfavourable pharmacodynamics.

Introduction

The major physiological ligands that activate platelets in haemostasis and thrombosis signal through G protein-coupled and tyrosine kinase-linked receptors. The former includes receptors for thrombin (PAR1, PAR4), thromboxane A_2 (TP) and ADP ($P2Y_1$, $P2Y_{12}$), and the latter receptors for collagen/fibrin (GPVI), podoplanin (CLEC-2), von Willebrand Factor (GPIb-IX-V) and fibrinogen (integrin αIIbβ3)[1,2].

GPVI is a receptor for collagen and fibrin which forms a complex with the Fc receptor □-chain (FcR□)[2-4]. GPVI triggers powerful platelet activation through Src, Syk and Tec family tyrosine kinases leading to activation of PLC□2[5]. GPVI is expressed exclusively on platelets and the platelet precursor cell the megakaryocyte[6]. Mice deficient in GPVI have a minor increase in tail bleeding times but fail to form occlusive thrombi in a $FeCl_3$ injury arterial thrombosis assay[7]. Patients homozygous for an insertion that introduces a stop codon and prevents expression of the immunoglobulin receptor on the platelet surface have a relatively mild bleeding diathesis[8], although they are too few in number to know if they are protected from thrombosis.

Bruton's tyrosine kinase (Btk) is a member of the Tec family of tyrosine kinases and mediates phosphorylation and activation of PLC□2 downstream of GPVI and the B cell antigen receptor. The irreversible Btk inhibitor ibrutinib has been introduced in the clinic for treatment of B cell malignancies but has been reported to increase rates of major haemorrhage in a sub-group of patients[9,10]. The increase in bleeding has been attributed to loss of platelet activation by GPVI[11-13] and GPIb[11], with the inhibition of the two receptors having been shown to correlate[14].

In contrast to treatment with ibrutinib, patients with X-linked Agammaglobulinemia (XLA) do not bleed excessively[15]. XLA is caused by mutations in the Btk gene that result in loss or reduction in Btk expression, or expression of a non-functional protein. A potential explanation for this discrepancy is that ibrutinib blocks activation of platelets by both Btk and the closely related kinase Tec. Tec is expressed in human and mouse platelets, and has been shown to support PLC□2 activation in mouse platelets[16]. Interestingly, major haemorrhage is not seen with the structurally related Btk inhibitor, acalabrutinib, despite also inhibiting Btk by covalent modification of C481[9,17]. It has been postulated that this is due to its greater selectivity to Btk over Tec in comparison to ibrutinib[17,18].

In the present study we have compared the inhibitory effects of ibrutinib and acalabrutinib on platelet activation and protein phosphorylation by GPVI alongside *ex vivo* studies on patients prescribed the two inhibitors, as well as on XLA patients.

Methods

Reagents

Details on the source of reagents and chemical analyses can be found in the

supplemental information.

Light transmission aggregometry (LTA)

Aggregation was measured in siliconised glass vials at 37°C in a Model 700 aggregometer (ChronoLog, Havertown, PA) with stirring at 1200 rpm. Platelets were warmed to 37°C for 5 min before experimentation. Platelets were pre-incubated with ibrutinib, acalabrutinib or DMSO vehicle for 5 min prior to agonist addition unless otherwise stated. Results were averaged and IC_{50} values were calculated from these data.

Protein phosphorylation

Washed platelets were pre-treated with 9 µM eptifibatide to block integrin αIIbβ3 activation. Agonists were added while stirring at 1200 rpm in an aggregometer at 37°C for 180 sec unless stated otherwise. Stimulations were performed in the presence of ibrutinib (17 nM - 7 µM), acalabrutinib (50 nM – 200 µM) or vehicle (DMSO). For whole cell lysate experiments; activation was terminated with 5X SDS reducing sample buffer. For immunoprecipitation; $8x10^8$/mL platelets were used and reactions were terminated by addition of 2X ice-cold Nonidet P-40 lysis buffer containing the protease inhibitors sodium orthovanadate (5 mM), leupeptin (10 µg/mL), AEBSF (200 µg/mL), aprotinin (10 µg/mL) and pepstatin (1 µg/mL). Platelet lysates were precleared, and detergent-insoluble debris was discarded. An aliquot was dissolved with SDS sample buffer for detection of total tyrosine phosphorylation. Lysates were incubated with either the indicated antibodies and protein A- or protein G-Sepharose. Lysates were separated by SDS-PAGE, electro-transferred, and Western blotted. Western blots were imaged using ECL autoradiography film. For analysis of levels of phosphorylation, Western blot films were scanned and band intensity measured using ImageJ 1.5 with values normalised to basal levels. Results were averaged and IC_{50} values were calculated from these data.

Other

Details on methods for blood sampling, platelet preparation, granule release, $[Ca^{2+}]_i$ mobilisation, measurement of platelet adhesion under flow, cell lines, plasmids, transfections and the luciferase assay can be found in the supplemental information.

Statistical analysis

All data are presented as mean ± standard error of the mean (SEM) with statistical significance taken as $p < 0.05$ unless otherwise stated. Statistical analyses, unless otherwise specified, were performed using one-way ANOVA with a Bonferroni post-test. *Ex vivo* platelet aggregation optical densities were compared using a one-way

ANOVA with Tukey's multiple comparison test. Correlation of aggregation and tyrosine phosphorylation was assessed using Pearson's correlation coefficient. Statistical analysis of the IC_{50} values was performed using Welch's t-test. All statistical analyses were performed using GraphPad Prism 7.

Ethical Approval

Ethical approval for collecting blood from patients and healthy volunteers was granted by the National Research Ethics Service (10/H1206/58) and Birmingham University Internal Ethical Review (ERN_11-0175) respectively. Work on HLA patients has ethical approval via the University of Birmingham HBRC 16-251 Amendment 1.

Results

Inhibition of GPVI-induced platelet aggregation by high concentrations of ibrutinib is reversible

Ibrutinib is 97% plasma protein bound and unbound levels reach approximately 0.5 μM in patients[11]. At this concentration, ibrutinib has been shown to block GPVI-induced platelet aggregation[12,19]. If this is due to inhibition of Btk and other Tec kinases then the inhibition should be irreversible and time-dependent (i.e. inhibition should increase with time). To test this, platelets were treated with a concentration of ibrutinib that causes complete inhibition of GPVI-mediated aggregation in washed platelets before washout of ibrutinib and stimulation with the GPVI-specific agonist collagen-related-peptide (CRP). Platelets showed almost full recovery on washout demonstrating that the inhibitory effect is not due solely to covalent modification of Btk or Tec (Figure 1A and 1B). In support of this, incubation for ≥30 sec in washed platelets with a high concentration of ibrutinib (700 nM) was sufficient to block aggregation to a high dose of CRP (Figure 1C). However, at a lower concentration, ibrutinib (70 nM) caused a time-dependent delay in aggregation to a high concentration of CRP that was apparent at incubation times of ≥ 5 min (Figure 1D and 2Ai). This concentration of ibrutinib also caused a reduced response to a sub-maximal concentration of CRP (Supplementary Figure 2A). The time-dependent delay is consistent with an irreversible action and contrasts with the rapid onset of inhibition observed at the high concentration of ibrutinib. A similar set of observations were seen in washed platelets stimulated by collagen (Supplementary Figure 1A). Similar results were also seen in the presence of 0.3% BSA which was used in case the results were influenced by adsorption of ibrutinib to the surface of the aggregometer tube (Supplementary Figure 1B).

Platelet secretion and Ca^{2+} mobilisation play key roles in platelet activation. Consistent with the results for aggregation, low (70 nM) and high (700 nM) concentrations of ibrutinib have no effect or block ATP secretion to a high

concentration of CRP, respectively (Figure 2Bi and 2Biii). Similarly, the peak Ca^{2+} concentration to a high concentration of CRP was not altered in the presence of a low concentration of ibrutinib (70 nM) but was markedly reduced by a high concentration (700 nM). The dose response curve for inhibition of aggregation was similar to that for loss of Ca^{2+} mobilisation (Figure 2Bii and 2Biii) and was not affected by the presence of the cyclooxygenase inhibitor indomethacin (Supplementary Figure 1D). There was no statistical difference between the IC_{50} of ibrutinib for secretion, aggregation or Ca^{2+} mobilisation.

Taken together these results show that ibrutinib has two distinct effects on platelet activation by CRP. At a low concentration (70 nM), ibrutinib delays but does not inhibit activation, whereas at a tenfold higher concentration of ibrutinib (700 nM) activation is blocked. The latter action is reversible indicating that it is not mediated by covalent modification of Btk or other Tec kinases.

Low dose ibrutinib blocks Btk but not Tec

The concentration response curve to ibrutinib on tyrosine phosphorylation was investigated in washed platelets in the same conditions as for the platelet function studies above. CRP induced robust tyrosine phosphorylation in whole cell lysates which was dose-dependently inhibited by ibrutinib. Correspondingly with the results for aggregation, this inhibitory effect of ibrutinib on global tyrosine phosphorylation was also reversible on washout (Figure 3Ai). Using phosphospecific antibodies, we were able to see that the inhibition of Src Y418 (which lies upstream of Btk) was also reversible but that autophosphorylation of Btk at Y223 and Btk substrates PLC□2 Y753 and Y1217[11, 20] were irreversible (Figure 3Ai-ii).

A detailed analysis of the dose response to ibrutinib on a wider range of proteins in the GPVI signalling cascade was investigated using further phosphospecific antibodies (Figure 3Bi). Autophosphorylation of Btk and downstream PLC□2 was reduced to basal levels by a low dose of ibrutinib (70 nM) (Figure 3Bii). In contrast, phosphorylation of Btk on Y551, which is mediated by Src family kinases[21], and proteins that lie upstream of Btk, namely Src Y418, Syk Y525/6, SLP-76 Y145 and LAT Y200, was not altered (Figure 3Biii-iv). Inhibition of phosphorylation of Src on its activation site, Y418, was observed at a tenfold higher concentration of ibrutinib (Figure 3Biv) and shown to correlate with inhibition of aggregation (Pearson's correlation coefficient 0.959). Inhibition of whole cell phosphorylation and phosphorylation of Syk Y525/6, SLP-76 Y145, Btk Y551 and LAT Y200 was seen at 7 μM ibrutinib which is tenfold higher than the maximal concentration in patients (Figure 3Bii and 3Biii). Where calculatable, the IC_{50} values for each phosphorylation event are included in Supplementary Table 1. Blockade of Btk pY223 and PLC□2 phosphorylation by 70 nM ibrutinib was also observed with lower concentrations of CRP or in the absence of the integrin αIIbβ3 blocker, eptifibatide (Supplementary Figure 2Aiv and 2B). There was no significant increase in phosphorylation of PLC□2 up to 180 sec in response to CRP in the presence of 70 nM ibrutinib (Supplementary Figure 2Ci-iii).

Due to the absence of phosphospecific antibodies for the Btk related Tec family kinase, Tec, the effect of ibrutinib on Tec phosphorylation was investigated following immunoprecipitation and re-probing with the antiphosphotyrosine mAb 4G10. The effect of ibrutinib was biphasic with partial blockade at 170 nM and full blockade observed at 7 μM (Figure 3C).

These results demonstrate that a concentration of 70 nM ibrutinib is sufficient to block Btk at its autophosphorylation site and on PLC□2 on Y753, Y759 and Y1217 and that this effect is irreversible. At this concentration of ibrutinib, aggregation to a high concentration of CRP is delayed but is not blocked. At a 10-20 fold greater concentration, ibrutinib reversibly blocks aggregation in parallel with reversible loss of phosphorylation of Src on Y418. Reversible inhibition of tyrosine phosphorylation of other proteins is seen at a 100-fold higher concentration than that required for blockade of Btk. Ibrutinib causes biphasic inhibition of phosphorylation of Tec, with inhibition occurring at 3-5 fold higher concentrations than required to block phosphorylation of Btk on Y223, and full blockade at a 100 fold higher concentration. These results are consistent with loss of Tec autophosphorylation at 170 nM of ibrutinib and loss of phosphorylation on the activation site by higher concentrations.

Low dose ibrutinib (70 nM) has no effect on platelet adhesion and aggregation to collagen under flow

The relevance of the observation that aggregation is delayed but not blocked to high concentrations of CRP and collagen was addressed using flow studies where GPVI functions in conjunction with other tyrosine kinase-linked receptors that also signal via Btk, namely GPIb and integrin αIIbβ3. To ensure that a known degree of Btk blockade was achieved, washed platelets were incubated with ibrutinib at a concentration sufficient to fully and irreversibly inhibit Btk kinase activity (70 nM). Inhibition of Btk autophosphorylation was confirmed by a delay in aggregation in response to CRP (Figure 4A) and by measurement of phosphorylation (not shown). Following incubation, platelets were reconstituted with autologous red blood cells and platelet poor plasma and flowed over collagen at arterial shear rates. Adhesion of ibrutinib treated platelets was unchanged when compared to vehicle treated platelets (Figure 4B).

Btk-specific concentrations of ibrutinib block GPVI mediated aggregation in patients with XLA

The B cell immunodeficiency XLA is caused by mutations in the Btk gene. Using knowledge of patient mutations (Supplementary Table 2), and an antibody to the N-terminus of Btk, we selected unrelated patients lacking Btk protein to test for off-target effects of ibrutinib (Figure 5Ai). Strikingly, the concentration response curve for inhibition of CRP-induced aggregation by ibrutinib was shifted to the left in the XLA patients when compared to healthy donors (Figure 5Aii-iii), whereas the curve for inhibition of PLC□2 phosphorylation was unchanged (Figure 5Aiv). Since the only known difference between XLA patients and controls is the absence of Btk, this demonstrates an off-target effect of ibrutinib that is unmasked in the absence of Btk

protein. This off-target action occurs over a similar concentration range to that required for inhibition of Btk. The GPCR agonists ADP and PAR1 peptide stimulated robust aggregation in XLA patients, as previously demonstrated[16] (not shown).

One possible explanation for the increased sensitivity of XLA patients to ibrutinib relative to controls is that Btk also functions as an adapter protein in the GPVI signalling pathway (as the only known difference in these two groups is Btk protein). To investigate this, we transfected Btk-deficient DT40 chicken B cells with GPVI and its signalling partner, FcR□, in the presence of wild type (WT) or kinase-dead (KD) Btk. Importantly, these cells express PLC□2 but do not express other Tec family kinases[22,23]. The K430E mutant of Btk has been previously reported to lack kinase activity[24]. Cells lacking Btk or GPVI were unresponsive to collagen. Cells transfected with WT or KD Btk reconstituted NFAT signalling to a similar degree, although there was a slight (Figure 6A-B) demonstrating that Btk also functions as an adapter protein in the GPVI signalling pathway. Low dose ibrutinib had no effect on cells transfected with WT or KD Btk whereas high dose ibrutinib blocked NFAT signalling in both WT and KD transfected cells (Figure 6C).

Together these results demonstrate that Btk functions as an adapter protein, as well as a kinase, in XLA platelets and in transfected DT40 cells.

Acalabrutinib inhibits Btk Y223 phosphorylation and platelet aggregation, secretion and Ca^{2+} mobilisation by GPVI

Studies were extended to a second generation Btk inhibitor, acalabrutinib, which, like ibrutinib, irreversibly binds to Btk at C481 and is highly plasma protein bound. Acalabrutinib has a higher selectivity over other tyrosine kinases relative to ibrutinib, including Src, Syk and Tec[25], but a five-fold lower IC_{50} for Btk[17]. In patients the mean peak free drug concentration of acalabrutinib is 1.3 μM[17].

Acalabrutinib has a similar, dose-dependent effect on platelet aggregation to that of ibrutinib. At a concentration of 2 μM in washed platelets, acalabrutinib induced a slight delay in aggregation (Supplementary Figure 3A) but had no effect on the overall magnitude of response (Figure 7Aii). The difference in the dose-dependency relative to ibrutinib is consistent with the lower IC_{50} of acalabrutinib for Btk. Similar to ibrutinib, inhibition of platelet aggregation by CRP occurs at acalabrutinib concentrations that are one order of magnitude higher than those which cause a delay in aggregation; and the curves for inhibition of ATP secretion and Ca^{2+} mobilisation lie slightly to the left of that for aggregation (Supplementary Figure 3A-E). As with ibrutinib, acalabrutinib blocked tyrosine phosphorylation of Btk on Y223 and PLC□2 on Y759 and Y1217 at a concentration (2 μM) that caused a delay in onset but no reduction in aggregation (Figure 7Ai and ii). Higher concentrations of acalabrutinib up to 200 μM had no effect on phosphorylation of Src Y418, Syk Y525/6 and LAT Y200 but caused a small reduction in phosphorylation of Btk Y551 and SLP-76 Y145 (Figure 7Ai and 7Aiii – iv). Interestingly, acalabrutinib also caused

a biphasic inhibition of Tec phosphorylation with partial inhibition observed at approximately 1 µM and full blockade at 200 µM (Figure 7B). The IC_{50} values for each phosphorylation event are included in Supplementary Table 1. Concentrations of acalabrutinib that blocked phosphorylation of Btk in platelets had no effect on NFAT activation by CRP in DT40 cells transfected with WT or KD Btk (Figure 7C).

Allowing for the fact that acalabrutinib has a 5-fold lower potency for Btk these results are in line with those for ibrutinib.

GPVI-mediated platelet aggregation is blocked *ex vivo* in patients taking ibrutinib, but not acalabrutinib

We investigated the effect of ibrutinib and acalabrutinib in patients with Chronic Lymphoid Leukaemia (CLL) taking ibrutinib 420 mg once daily, acalabrutinib 100 mg twice daily or a non-Btk targeting control chemotherapy regimen. GPVI-induced platelet aggregation is blocked in the PRP of patients taking ibrutinib but is not blocked in patients taking acalabrutinib or in the control group despite complete inhibition of autophosphorylation of Btk pY223 and its downstream substrate PLC□2 at pY1217 by both inhibitors (Figure 5Bi-iv). Platelet aggregation induced by the GPCR agonists, ADP and PAR1 peptide, was not altered in the patients taking either inhibitor (not shown).

Discussion

In this study we show that (i) irreversible blockade of Btk by ibrutinib and acalabrutinib delays but does not block platelet aggregation by high concentrations of GPVI agonists; (ii) blockade of GPVI-mediated aggregation by ibrutinib and acalabrutinib occurs at a concentration 1-2 orders of magnitude higher than is required to block Btk due to an off-target action which is reversible; (iii) the ratio between inhibition of Btk kinase activity and platelet aggregation by GPVI is the same for ibrutinib and acalabrutinib; (iv) clinically relevant concentrations of ibrutinib but not acalabrutinib block activation of platelets by GPVI; (v) platelet adhesion and aggregation under flow conditions is maintained following inhibition of Btk; (vi) Btk supports platelet activation by GPVI by acting as an adapter protein and as a tyrosine kinase; and (vii) ibrutinib blocks platelet aggregation in XLA patients at concentrations that block Btk.

These results show that platelets, in which Btk kinase function and downstream PLC□2 phosphorylation have been blocked, have a slight delay in aggregation in response to high concentrations of GPVI ligands, while platelet adhesion and aggregation under arterial flow conditions are unaltered. These observations, together with reports that patients with XLA or those treated with acalabrutinib do not experience major bleeding[15,17], provide powerful evidence that inhibition of Btk does not give rise to major bleeding. The major bleeding observed in patients treated with ibrutinib relative to acalabrutinib is due to the differential dosing regimens of the two

Btk inhibitors, with the clinical dose of ibrutinib blocking activation of platelets by GPVI due to one or more off-target effects.

The conclusion that inhibition of Btk does not give rise to major bleeding on treatment with ibrutinib contrasts with the conclusion of the studies by Levade *et al.*[11] and Bye *et al.*[13]. Levade *et al.*[11] demonstrated a close correlation between inhibition of autophosphorylation of Btk at Y223 and aggregation in GPVI activated platelets. While we are unable to explain this in light of the present observations, we note that Levade *et al.*[11] also reported that phosphorylation of PLC□2 at Y753, which is mediated by Btk, was inhibited at a tenfold lower concentration of ibrutinib as is seen in the present study. Bye *et al.*[13] used a single, supramaximal concentration of ibrutinib which also blocks Src phosphorylation for their biochemical and flow based assays. The determination of full concentration response curves in the present study has highlighted the mismatch between inhibition of Btk and loss of platelet aggregation, and has provided evidence that the bleeding diathesis that is seen in some ibrutinib-treated patients is due to off-target effects.

An unexpected observation in the present study is that platelets are able to aggregate to a high dose of CRP despite the absence of detectable PLC□2 phosphorylation. One explanation for this is that Btk also supports activation of PLC□2 as an adapter protein as shown by the observation that transfection of kinase dead Btk restores GPVI signalling in DT40 cells. A similar result has been previously shown for Btk in B cell receptor signalling[24,26]. This is in keeping with previous studies that show that phosphorylation of PLC□2 at Y1217 is not required for its enzymatic activity in Ramos cells[27].

We were surprised to find that platelets from XLA patients, who lack Btk protein, have increased susceptibility to ibrutinib relative to platelets from controls. The only known difference between the XLA patients and controls in the presence of ibrutinib is the absence of Btk protein, although this could also change the balance of activatory and inhibitory phosphorylations within the GPVI signalling cascade. Further, the absence of Btk renders aggregation of these platelets critically dependent on PLC□2 phosphorylation in contrast to controls. The target for ibrutinib which gives rise to inhibition of aggregation in the XLA patients is not known. There are several kinases that are inhibited by ibrutinib over a similar concentration range to that for inhibition of Btk[18]. Within this group only Csk is known to be expressed in platelets[28].

We have shown that blockade of GPVI-mediated platelet aggregation by ibrutinib is reversible, which contrasts with the irreversible blockade of Btk and Tec[18]. The reversibility provides evidence that blockade is not mediated by inhibition of Tec family kinase as has been previously postulated[9,11,17] as Tec also has a cysteine residue in its ATP binding domain analogous to C481 on Btk. This is further supported by the observation that ibrutinib mediated blockade of NFAT signalling in DT40 cells, which lack Tec, follows a similar pattern as that for platelet aggregation; namely no effect at low doses with blockade at high doses. For ibrutinib, we have

shown that inhibition of aggregation correlates strongly with loss of phosphorylation at Src Y418. However, this is not altered by acalabrutinib demonstrating an as yet unidentified off-target action. Bye et al[13] also show that ibrutinib dose dependently inhibits phosphorylation of Src Y418. However, in a different study they report that both low dose ibrutinib and acalabrutinib potentiate Src Y418 phosphorylation[29]. We were not able to replicate this latter finding.

We have shown that, despite acalabrutinib's more favourable selectivity to Btk over other Src, Syk and Tec kinases in *in vitro* kinase assays, the window between Btk inhibition and blockade of GPVI-induced aggregation *in vitro* is similar to that of ibrutinib. Despite this, acalabrutinib, but not ibrutinib, fails to block GPVI-mediated platelet activation *ex vivo*. We propose that this is because of the differential dosing and pharmacodynamics of the two Btk inhibitors. Acalabrutinib is used at a dose of 1.5 mg/kg twice daily[17,30] and ibrutinib at a single daily dose of 6 mg/kg in CLL or 8 mg/kg in Mantle Cell Lymphoma (MCL). Pharmacokinetic studies have shown that ibrutinib achieves Btk occupancy of >95% at doses of 2.5 mg/kg but that doses of 6 mg/kg are required to maintain this over 24 hours[31]. Acalabrutinib at 1.5 mg/kg twice daily also achieves full Btk occupancy over 24 hours[17]. The peak unbound plasma concentration of ibrutinib in patients is 0.5 μM[11] and that of acalabrutinib 1.3 μM[17]. The initial and terminal half-lives of ibrutinib are 2-3 hours and 4-8 hours respectively[31]. The half-life of acalabrutinib is 1 hour[17]. Despite the peak concentration of acalabrutinib being approximately 2-fold higher than the concentration of ibrutinib, the 5-fold lower potency of acalabrutinib as an inhibitor of Btk[30] means that, in potency terms, it is dosed at a lower level consistent with the lack of inhibition of GPVI. This implies that ibrutinib could be used at a lower concentration to achieve Btk blockade. Indeed, there is retrospective clinical evidence that doses less than 6 mg/kg are as effective as 6 mg/kg at treating CLL[32] and a prospective clinical trial using doses as low as 2.5 mg/kg is being undertaken[33].

It is important to consider the incidence of minor and major bleeding in patients taking ibrutinib for CLL or at the higher dose for MCL. In reported studies involving patients treated with ibrutinib for MCL, minor and major bleeding is seen in 9-15% and 1-5% of patients respectively[34,35,36]. The study with the largest cohort of MCL patients reports a major haemorrhage rate of 5%. This is comparable to the 4-8% major haemorrhage rate seen in patients taking ibrutinib for CLL[9]. Thus, there is no increase in bleeding rates with higher doses of ibrutinib. This implies that the inhibitory effect of 420mg ibrutinib on platelets is at a physiologic maximum.

During the writing of this manuscript, Bye *et al.* reported thrombus instability on collagen in a flow adhesion assay in blood treated *in vitro* with high doses of ibrutinib and *ex vivo* in patients treated with ibrutinib[29]. This is consistent with our findings that Btk kinase function is not required for platelet adhesion to collagen under flow, but that off target effects of ibrutinib seen with higher doses mediate this inhibition. They

also report complete blockade of platelet aggregation to supramaximal concentrations of collagen in patients receiving ibrutinib or acalabrutinib[29] in contrast to the findings of this study. Bye *et al.* used the Optimul 96 well microtitre assay to measure aggregation rather than the widely used light transmission aggregometry (LTA). We have shown that Optimul is a more sensitive assay than LTA[37,38]. We suggest that the delay in onset of aggregation observed using LTA by concentrations of ibrutinib or acalabrutinib that just block Btk manifest as complete blockade in the Optimul assay. Bye *et al*. also conclude that the increased bleeding observed with ibrutinib is due to blockade of Src family kinases (SFK)[29]. We agree that bleeding caused by ibrutinib is due to off-target actions, and that acalabrutinib has a greater selectively to Btk over SFK relative to ibrutinib. However, our results show that a similar fold increase in the concentration of ibrutinib and acalabrutinib causes inhibition of platelet aggregation to CRP but without concomitant SFK blockade in the acalabrutinib treated platelets. Thus, the off-target action of ibrutinib and acalabrutinib that inhibits aggregation cannot be explained solely by differential blockade of SFKs.

The results of our study explain the lack of major bleeding side effects experienced by patients taking acalabrutinib relative to ibrutinib and suggest that the bleeding side effect of ibrutinib can potentially be abolished by reducing the dose. Further, this study also shows that the bleeding caused by ibrutinib is not due to an irreversible action. This predicts that the GPVI blockade wears off over a period of 24 hours as the drug is cleared[31]. We hypothesise that, in the event of a major bleed, there may be no need to use expensive and potentially harmful platelet transfusions to correct the signalling deficit. Each clinical scenario should be judged on its own merits, however, and individual clinician discretion is crucial.

In conclusion; the present study shows that inhibition of Btk kinase activity causes only partial inhibition of GPVI signalling in platelets and provides evidence that Btk supports GPVI signalling by functioning as an adapter protein as well as a kinase. The excessive bleeding induced by ibrutinib relative to acalabrutinib is likely to reflect a non-Tec family kinase off target inhibitory effect of ibrutinib, probably on Src.

Acknowledgements

This work was supported by the British Heart Foundation (BHF) Programme Grants (RG/13/18/30563), BHF clinical fellowship to PLRN (FS/17/20/32738), AMS springboard grant to AYP (SBF002\1099) and BHF studentship to ATH, the University of Birmingham's Institute of Translation Medicine and Institute of Cardiovascular Sciences; SPW holds a BHF Chair (CH03/003).

We would like to thank Alex Bye and Jon Gibbins for their expertise on the Ca^{2+} mobilisation assay. We would like to thank Vicky Simms, Natalie Poulter and Steve Thomas for their help with the flow adhesion assay. We would like to thank Mark Crowther, Nick Pemberton, Salim Shafeek, Kate Arthur, Gaynor Pemberton, Lesley Candlin and Rebekah Hart at Worcestershire Royal Hospital, Shankara Paneesha,

Aarnoud Huissoon, Hayley Clifford, Alison Hardy and Melanie Kelly at Birmingham Heartlands Hospital and Tina McSkeane, Gillian Marshall and Michelle Harry at the Queen Elizabeth Hospital for provision of patient samples. We would like to thank Andrew Wilkinson and Robert Neely from the School of Chemistry at the University of Birmingham for their help with the chemical analysis of ibrutinib and acalabrutinib.

Author contributions

PLRN, CEH, MGT, GP and SPW conceived, planned and wrote the study. Additionally, PLRN, SW, CEH, SHN, CNW and MRT performed experiments. JDM provided key reagents. PLRN, CEH and SPW wrote the manuscript. MGT, SW, ATH, MRT, SJM, AYP and GP critically appraised the manuscript.

Conflict of interest Disclosures

The authors declare no competing financial interests.

References:

1. Li Z, Delaney MK, O'Brien KA, Du X. Signalling During Platelet Adhesion and Activation. Arterioscler. Thromb Vasc Biol. 2010;30(12):2341–2349.
2. Alshehri OM, Hughes CE, Montague S, et al. Fibrin activates GPVI in human and mouse platelets. Blood. 2015;126(13):1601–1608.
3. Nieswandt B. Platelet-collagen interaction: is GPVI the central receptor? Blood. 2003;102(2):449–461.
4. Mammadova-Bach E, Ollivier V, LOYAU S, et al. Platelet glycoprotein VI binds to polymerized fibrin and promotes thrombin generation. Blood. 2015;126(5):683–691.
5. Watson SP, Herbert JMJ, Pollitt AY. GPVI and CLEC-2 in hemostasis and vascular integrity. J Thromb Haemost. 2010;8(7):1456–1467.
6. Jandrot-Perrus M, Busfield S, Lagrue AH, et al. Cloning, characterization, and functional studies of human and mouse glycoprotein VI: a platelet-specific collagen receptor from the immunoglobulin superfamily. Blood. 2000;96(1):1798–1807.
7. Bender M, Hagedorn I, Nieswandt B. Genetic and antibody-induced glycoprotein VI deficiency equally protects mice from mechanically and FeCl3-induced thrombosis. J Thromb Haemost. 2011;9(7):1423–1426.
8. Nurden AT, Nurden P. Congenital platelet disorders and understanding of platelet function. Br J Haematol. 2013;165(2):165–178.
9. Shatzel JJ, Olson SR, Tao DL, et al. Ibrutinib-associated bleeding: pathogenesis, management, and risk reduction strategies. J Thromb

Haemost. 2015;38(1):42–49.

10. Caron F, Leong DP, Hillis C, Fraser G, Siegal D. Current understanding of bleeding with ibrutinib use: a systematic review and meta-analysis. Blood Adv. 2017;1(12):772–778.

11. Levade M, David E, Garcia C, Laurent P, Payrastre B. Ibrutinib treatment affects collagen and von Willebrand factor-dependent platelet functions. Blood. 2014;124(26):3991–3995.

12. Kamel S, Horton L, Ysebaert L, et al. Ibrutinib inhibits collagen-mediated but not ADP-mediated platelet aggregation. Leukemia. 2015;29(4):783–787.

13. Bye AP, Unsworth AJ, Vaiyapuri S, Stainer AR, Fry MJ, Gibbins JM. Ibrutinib Inhibits Platelet Integrin αIIbβ3 Outside-In Signalling and Thrombus Stability But Not Adhesion to Collagen. Arterioscler Thromb Vasc Biol. 2015;35(11):2326-2335.

14. Kazianka L, Drucker C, Skrabs C, et al. Ristocetin-induced platelet aggregation for monitoring of bleeding tendency in CLL treated with ibrutinib. Leukemia. 2017;31(5):1117–1122.

15. Quek LS, Bolen J, Watson SP. A role for Bruton's tyrosine kinase (Btk) in platelet activation by collagen. Curr Biol. 1998;8(20):1137-1140.

16. Atkinson BT, Ellmeier W, Watson SP. Tec regulates platelet activation by GPVI in the absence of Btk. Blood. 2003;102(10):3592–3599.

17. Byrd JC, Harrington B, O'Brien S, et al. Acalabrutinib (ACP-196) in Relapsed Chronic Lymphocytic Leukemia. N Engl J Med. 2016;374(4):323–332.

18. Honigberg L, Smith AM, smith, et al. The Bruton tyrosine kinase inhibitor PCI-32765 blocks B-cell activation and is efficacious in models of autoimmune disease and B-cell malignancy. Proc Natl Acad Sci U S A. 2010;107(29):13075–13080.

19. Rushworth SA, MacEwan DJ, Bowles KM. Ibrutinib in Relapsed Chronic Lymphocytic Leukemia. N Engl J Med. 2013;369(13):1277–1279.

20. Watanabe D, Hashimoto S, Ishiai M, et al. Four tyrosine residues in phospholipase C-gamma 2, identified as Btk-dependent phosphorylation sites, are required for B cell antigen receptor-coupled calcium signalling. J Biol Chem. 2001;276(42):38595–38601.

21. Wahl MI, Fluckiger AC, Kato RM, et al. Phosphorylation of two regulatory tyrosine residues in the activation of Bruton's tyrosine kinase via alternative receptors. Proc Natl Acad Sci U S A. 1997;94(21):11526–11533.

22. Tomlinson MG, Kurosaki T, Berson AE, Fujii GH, Bolen JB. Reconstitution of Btk Signalling by the Atypical Tec Family Tyrosine Kinases Bmx and Txk*. J Biol Chem. 1999;274(19):13577–13585.

23. Takata M, Homma Y, Kurosaki T. Requirement of Phospholipase C-□2 Activation in Surgace Immunoglobulin M-induced B Cell Apoptosis. J Exp Med. 1995;182(4):907–914.

24. Tomlinson MG, Woods DB, McMahon M, et al. A conditional form of Bruton's tyrosine kinase is sufficient to activate multiple downstream signalling pathways via PLC Gamma 2 in B cells. BMC Immunol. 2001;2(4):1–12.

25. Wu J, Zhang M, Liu D. Acalabrutinib (ACP-196): a selective second-generation BTK inhibitor. J Hematol Oncol. 2016;9(1):1–4.

26. Salto K, Tolias KF, Abdelhafid S, et al. Btk Regulates PtdIns-4,5-P2 Synthesis: Importance for Calcium Signalling and PI3K Activity. Immunity. 2003;19:669–678.

27. Kim YJ, Sekiya F, Poulin B, Bae YS, Rhee SG. Mechanism of B-Cell Receptor-Induced Phosphorylation and Activation of Phospholipase C- 2. Mol Cell Biol. 2004;24(22):9986–9999.

28. Burkhart JM, Vaudel M, Gambaryan S, et al. The first comprehensive and quantitative analysis of human platelet protein composition allows the comparative analysis of structural and functional pathways. Blood. 2012;120(15):e73–e82.

29. Bye AP, Unsworth AJ, Desborough MJ, et al. Severe platelet dysfunction in NHL patients receiving ibrutinib is absent in patients receiving acalabrutinib. Blood Adv. 2017;1(26):2610–2623.

30. Covey T, Barf T, Gulrajani M, et al. Abstract 2596: ACP-196: a novel covalent Bruton's tyrosine kinase (Btk) inhibitor with improved selectivity and in vivo target coverage in chronic lymphocytic Leukemia (CLL) patients. Cancer Res. 2015;75(15 Supplement):2596–2596.

31. Advani RH, Buggy JJ, Sharman JP, et al. Bruton Tyrosine Kinase Inhibitor Ibrutinib (PCI-32765) Has Significant Activity in Patients With Relapsed/Refractory B-Cell Malignancies. J Clin Oncol. 2012;31(1):88–94.

32. Banerjee R, Timlin C, Fitzpatrick D, et al. Comparable outcomes in Chronic Lymphocytic Leukeemia patients treated with reduced dose ibrutinib: Results from a multi-center study. Haematologica. 2016;101(s1):56-57.

33. Bose P, Gandhi VV, Keating MJ. Pharmacokinetic and pharmacodynamic evaluation of ibrutinib for the treatment of chronic lymphocytic Leukeemia: rationale for lower doses. Expert Opin Drug Metab Toxicol. 2016;11:1–12.

34. Dreyling, M, Jurczak W, Silva RS, et al. Ibrutinib versus temsirolimus in patients with relapsed or refractory mantle-cell lymphoma: an international, randomised, open-label, phase 3 study. Lancet. 2016;387(10020):770-78.

35. Rule, S, Dreyling, M, Goy, A, et al. Outcomes in 370 patients with mantle cell lymphoma treated with ibrutinib: a pooled analysis from three open-label

studies. Br J Haematol. 2017;179(3):430-438.

36. Wang, ML, Rule S, Martin, P, et al. Targeting BTK with Ibrutinib in Relapsed or Refractory Mantle-Cell Lymphoma. N Eng J Med. 2013;369(6):507-516.

37. Lordkipanidzé M, Lowe GC, Kirkby NS, et al. Characterization of multiple platelet activation pathways in patients with bleeding as a high-throughput screening option: use of 96-well Optimul assay. Blood. 2014;123(8):e11-e22.

38. Chan, MV, Leadbeater, PD, Watson, SP, Warner TD. Not all light transmission aggregation assays are created equal: qualitative differences between light tramsission and 96-well plate aggregometry. Platelets. 2018 May 1:1-4. [Epub ahead of print]

39. Hughes CE, Pollitt AY, Mori J, et al. CLEC-2 activates Syk through dimerization. Blood. 2010;115(14):2947–2955.

40. Grynkiewicz G, Poenie M, Tsien RY. A New Generation of Ca2+ Indicators with Greatly Improved Fluorescence Properties**.** J Biol Chem. 2001;260(6):3440–3450.

41. Takata M, Kurosaki T. A Role for Bruton's Tyrosine Kinase in B Cell Antigen Receptor-mediated Activation of Phospholipase C-□2. J Exp Med. 1996;184(1):31–40.

42. Hughes CE, Sinha U, Pandey A, et al. Critical Role for an Acidic Amino Acid Region in Platelet Signalling by the HemITAM (Hemi-immunoreceptor Tyrosine-based Activation Motif) Containing Receptor CLEC-2 (C-type Lectin Receptor-2). J Biol Chem. 2013;288(7):5127–5135.

Figure Legends

Figure 1. Increasing ibrutinib incubation time has no effect on degree of inhibition of platelet aggregation and this inhibition is reversed by washing. (A) Representative traces of washed platelets at $4x10^8$/ml stimulated with CRP (10 µg/mL for 180 sec). Prior to addition of agonist, platelets were pre-incubated with either ibrutinib or vehicle (DMSO) for 5 min. Alongside, washed platelets at $4x10^8$/ml identically treated with either ibrutinib or vehicle were washed twice in Tyrode's buffer and platelets resuspended to $4x10^8$/mL; platelets were then stimulated with CRP (10 µg/mL for 180 sec). Data shown is representative of three identical experiments. (B) Mean data for (A) (n=3) analysed with one-way ANOVA. Results are shown as mean ± SEM. * $p < 0.05$. (C) Washed platelets ($4x10^8$/mL) were incubated with ibrutinib or vehicle (DMSO) for 30 sec - 60 min before being stimulated with CRP (10 µg/mL). The optical density (OD) of platelet suspensions was measured in a ChronoLog Model 700 aggregometer with stirring at 1200 rpm. Traces representative of three similar experiments are shown. (D) Delay in aggregation seen with ibrutinib treated washed platelets (n=3) analysed with one-way ANOVA. Results are shown as mean ± SEM. * $p < 0.05$.

Figure 2. Ibrutinib dose dependently inhibits GPVI-mediated platelet aggregation, ATP secretion and Ca^{2+} mobilisation. (A) (i) Representative traces showing effect of increasing doses of *in vitro* ibrutinib incubated for 5 min in washed platelets at $4x10^8$/ml. (ii) Ibrutinib dose response curves in washed platelets (n=7). (B) Representative traces showing effect of increasing doses if *in vitro* ibrutinib incubated in washed platelets at $4x10^8$/ml for 5 min on (i) ATP secretion and (ii) Ca^{2+} mobilisation in response to stimulation with CRP (10 µg/mL) for 180 sec. (iii) Ibrutinib dose response curves in washed platelets of ATP secretion (n=3) and Ca^{2+} mobilisation (n=3). The dose response curve for inhibition of washed platelet aggregation from (Aiii) is shown as a dotted line to enable comparison. Results are shown as mean ± SEM. All experiments were stimulated with CRP (10 µg/mL). For comparison of IC_{50}: ns = non-significant.

Figure 3. **Ibrutinib dose-dependently inhibits GPVI-mediated signalling.** (A) Eptifibatide (9 µM) treated washed human platelets ($4×10^8$/mL) were stimulated with CRP (10 µg/mL for 180 sec) followed by lysis with 5X SDS reducing sample buffer. Prior to addition of agonist, platelets were pre-incubated with either ibrutinib or vehicle (DMSO). Some platelets underwent two further washs step prior to addition of agonist. (i) Whole cell lysates were then separated by SDS-PAGE and Western blot with the stated antibodies for whole cell phosphorylation, kinases and proteins downstream of GPVI. Blots are representative of three experiments. (ii) Percentage tyrosine phosphorylation as compared to non-washed vehicle platelets was measured and is represented as the means ± SEM of three identical experiments. (Bi) Washed platelets were treated as in (A) but with a wider range of ibrutinib doses. (ii - iv) The percentage of tyrosine phosphorylation as compared to vehicle treated platelets was measured and is represented as the means ± SEM of four identical experiments. The dose response curve for inhibition of washed platelet aggregation from Figure 2Aii is shown as a dotted line to enable comparison. (C) Eptifibatide (9 µM) treated washed human platelets ($8×10^8$/mL) were stimulated with CRP (10 µg/mL for 180 sec) followed by lysis with 2X ice cold lysis sample buffer. Lysates were pre-cleared and Tec was immunoprecipitated before addition of SDS reducing sample buffer and separation by SDS-PAGE and Western blot with the anti-pY antibody 4G10. Membranes were stripped and then reprobed with the pan-Tec antibody. (i) Trace is representative of three identical experiments. (ii) The percentage of tyrosine phosphorylation as compared to vehicle treated platelets was measured and is represented as the means ± SEM of three identical experiments. * $p < 0.05$. ns = non-significant.

Figure 4. Low dose ibrutinib has no effect on platelet adhesion to collagen under flow. (A) Washed platelets ($10x10^8$/mL) we incubated with ibrutinib or vehicle (DMSO) for 5 min and stimulated with CRP (10 µg/mL). Representative trace (i) and mean data from three identical experiments (ii) show characteristic delay associated with inhibition of Btk autophosphorylation. (B) Platelets were reconstituted with autologous RBCs and PPP and flowed at arterial shear over collagen coated microcapillaries. (i) Representative Differential Interference Contrast (DIC) images are shown. (ii) Platelet coverage as percentage of vehicle treated platelets was calculated and is shown as mean ± SEM from three identical experiments. * $p < 0.05$, ns = non significant.

Figure 5. **XLA patients who lack Btk expression are more sensitive than healthy donors to ibrutinib inhibition of GPVI-mediated platelet aggregation. Ibrutinib, but not acalabrutinib, blocks GPVI-mediated platelets aggregation *ex vivo***. (A) Citrated blood was taken from XLA patients. (i) Whole cell lysates were then separated by SDS-PAGE and Western blot with the polyclonal N-terminal Btk antibody. PRP from XLA patients was stimulated with CRP (10 µg/mL) for 180 sec. (ii) Representative aggregation trace of XLA patients or healthy donor (HD). (iii) Ibrutinib dose response curves in washed platelets of XLA patients (n=4). Healthy donor responses from Figure 2Aiii are shown as a dotted line for comparison. (iv) Whole cell lysates were then separated by SDS-PAGE and Western blot with the phosphospecific antibody to PLC□2 Y1217 (n=3). XLA patient aggregation curve shown as dotted line for comparison. (B) Patients taking ibrutinib 420mg once daily, acalabrutinib 100mg twice daily or a control chemotherapy regime of Fludarabine (25mg/m^2 IV days 1-3), Cyclophosphamide (250mg/m^2 IV days 1-3) and Rituximab (375mg/m^2 IV day 1) (FCR) had citrated blood taken on day 28 of treatment cycle (2-3 hours post dose of Btk inhibitor). PRP from this blood was then stimulated with CRP (10 µg/mL) for 180 sec. (i) Representative trace. (ii) Mean and SEM from five, nine and three patients for FCR, ibrutinib and acalabrutinib respectively. (iii) Comparison of platelet counts in PRP from all patient groups. Statistical analysis was performed using a one way ANOVA with Tukey's multiple comparisons test, *$p < 0.05$, ns = not significant. (iv) Representative western blot from eptifibatide (9 µM) treated washed platelets (4×10^8/mL) from the same patients stimulated with CRP (10 µg/mL for 180 sec) followed by lysis with 5X SDS sample buffer and probed with Btk pY223 and PLC□2 pY1217 phosphospecific antibody.

Figure 6. Kinase dead Btk is sufficient for GPVI signalling. Btk deficient DT40 cells were transfected with either wild type (WT) or kinase dead (KD) Btk with or without GPVI/FcR□. All cells were transfected with a NFAT-luciferase reporter plasmid. Cells were stimulated with collagen (10 µg/mL) in the presence of serum. (A) Luciferase activity was measured and is shown as mean ± SEM of five identical experiments. (B) Representative western blot showing equal Btk expression in WT and KD transfected cells. (C) Cells were stimulated with collagen (10 µg/mL) in the presence or absence of ibrutinib (0.5 µM – 10 µM). Serum was excluded during stimulation to avoid plasma binding of the drugs. Luciferase activity between vehicle and drug treated samples was measured and is shown as the mean ± SEM of three independent experiments. * $p < 0.05$, ** $p < 0.01$.

Figure 7. **Acalabrutinib dose-dependently inhibits GPVI-mediated signalling.** （A） Eptifibatide (9 µM) treated washed human platelets (4×10^8/mL) were stimulated with CRP (10 µg/mL for 180 sec) followed by lysis with 5X SDS reducing sample buffer. Prior to addition of agonist, platelets were pre-incubated with either acalabrutinib or vehicle (DMSO). (i) Whole cell lysates were then separated by SDS-PAGE and Western blot with the stated antibodies for whole cell phosphorylation, kinases and proteins downstream of GPVI. Blots are representative of three experiments. (ii - iv) The percentage of tyrosine phosphorylation as compared to vehicle treated platelets was measured and is represented as the means ± SEM of three identical experiments. The dose response curve for inhibition of aggregation from Supplementary Figure 3D is shown as a dotted line to enable comparison. （B）

Eptifibatide (9 μM) treated washed human platelets (8×10^8/mL) were stimulated with CRP (10 μg/mL for 180 sec) followed by lysis with 2X ice cold lysis sample buffer. Lysates were precleared and Tec was immunoprecipitated before addition of SDS reducing sample buffer and separation by SDS-PAGE and Western blot with the anti-pY antibody 4G10. Membranes were stripped and reprobed with the pan-Tec antibody. Trace is representative of three identical experiments. (C) Btk deficient DT40 cells were transfected with either wild type (WT) or kinase dead (KD) Btk with or without GPVI/FcR□. All cells were transfected with a NFAT-luciferase reporter plasmid. Cells were stimulated with collagen (10 μg/mL) in the presence or absence of acalabrutinib (0.5-10 μM). Serum was excluded during stimulation to avoid plasma binding of the drugs. Luciferase activity between vehicle and drug treated samples was measured and is shown as the mean ± SEM of three independent experiments. ns = non-significant.

Figure 1

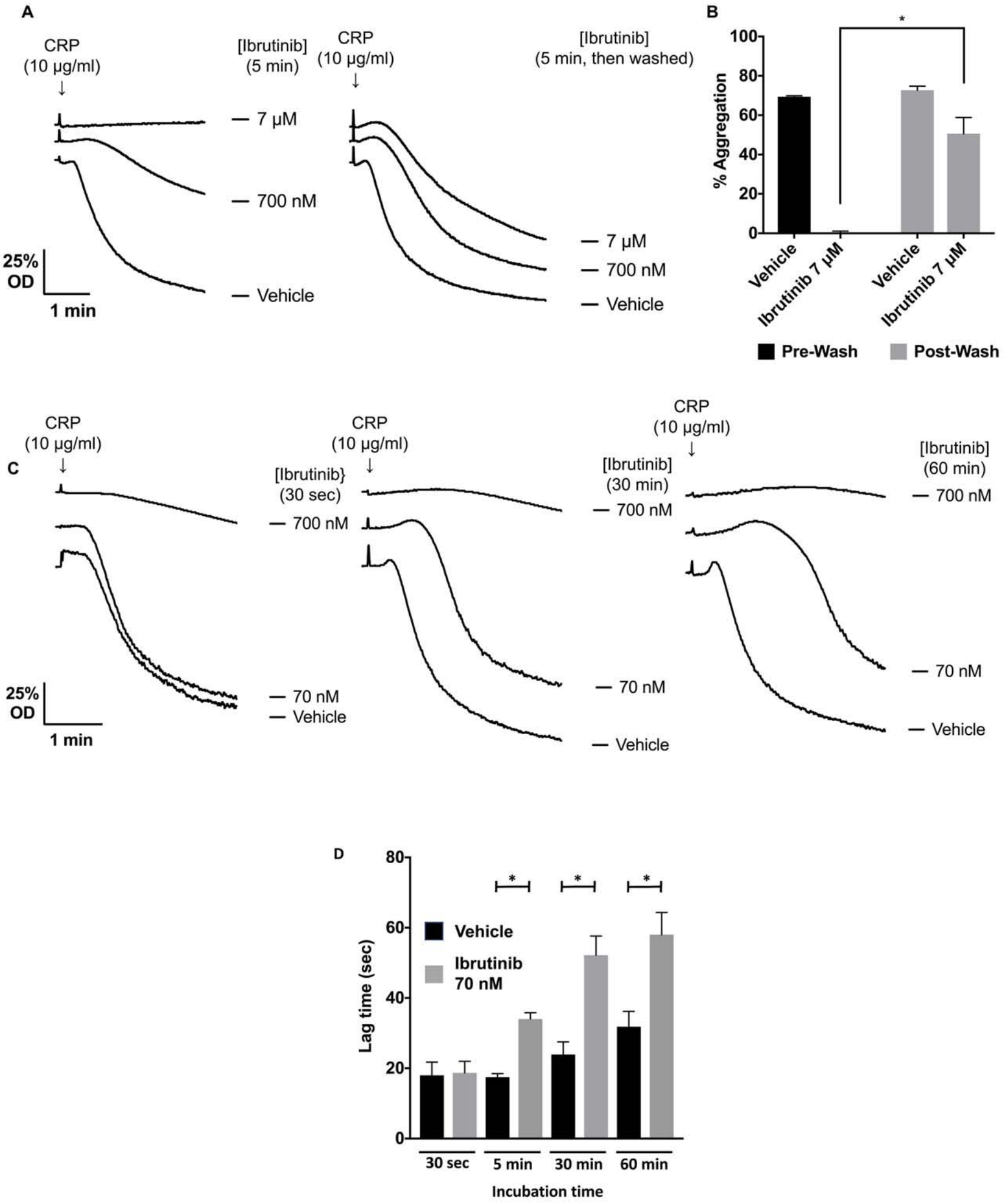
A
CRP
(10 µg/ml)
[Ibrutinib]
(5 min)
CRP
(10 µg/ml)
[Ibrutinib]
(5 min, then washed)
7 µM
700 nM
Vehicle
25%
OD
1 min
B
% Aggregation
100
80
60
40
20
0
*
Vehicle
Ibrutinib 7 µM
Vehicle
Ibrutinib 7 µM
Pre-Wash
Post-Wash
C
CRP
(10 µg/ml)
[Ibrutinib}
(30 sec)
CRP
(10 µg/ml)
[Ibrutinib]
(30 min)
CRP
(10 µg/ml)
[Ibrutinib]
(60 min)
700 nM
70 nM
Vehicle
25%
OD
1 min
D
Lag time (sec)
80
60
40
20
0
*
*
*
Vehicle
Ibrutinib
70 nM
30 sec
5 min
30 min
60 min
Incubation time

Figure 2

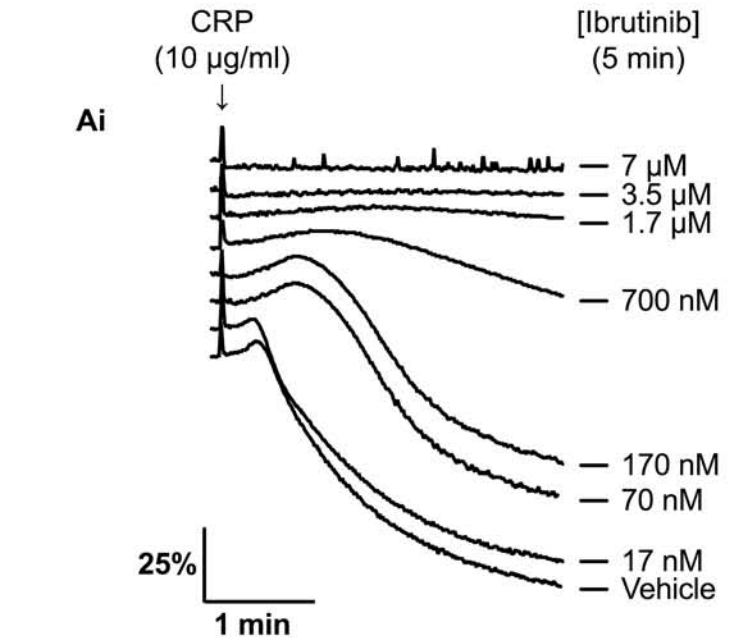
Ai
CRP
(10 µg/ml)
[Ibrutinib]
(5 min)
7 µM
3.5 µM
1.7 µM
700 nM
170 nM
70 nM
17 nM
Vehicle
25%
1 min

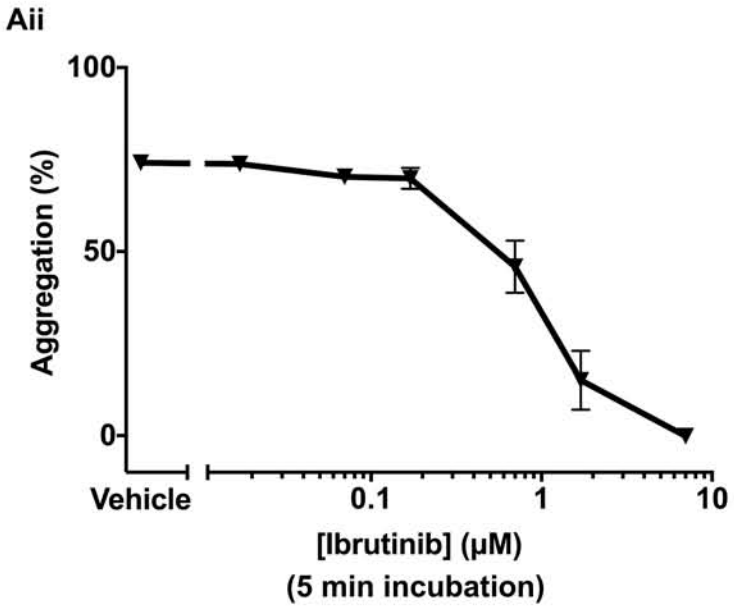
Aii
100
50
0
Aggregation (%)
Vehicle
0.1
1
10
[Ibrutinib] (µM)
(5 min incubation)

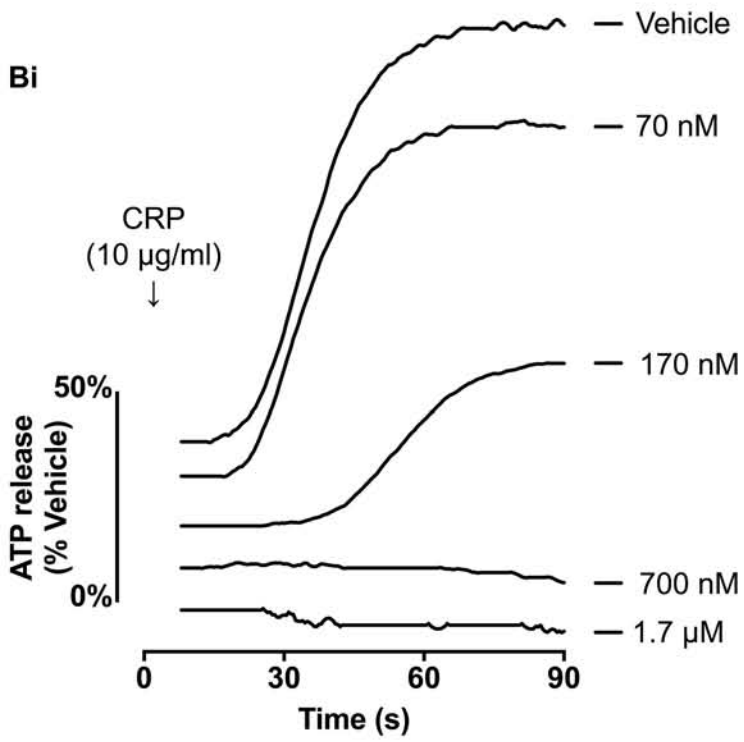
Bi
Vehicle
70 nM
CRP
(10 µg/ml)
170 nM
50%
0%
ATP release
(% Vehicle)
700 nM
1.7 µM
0
30
60
90
Time (s)

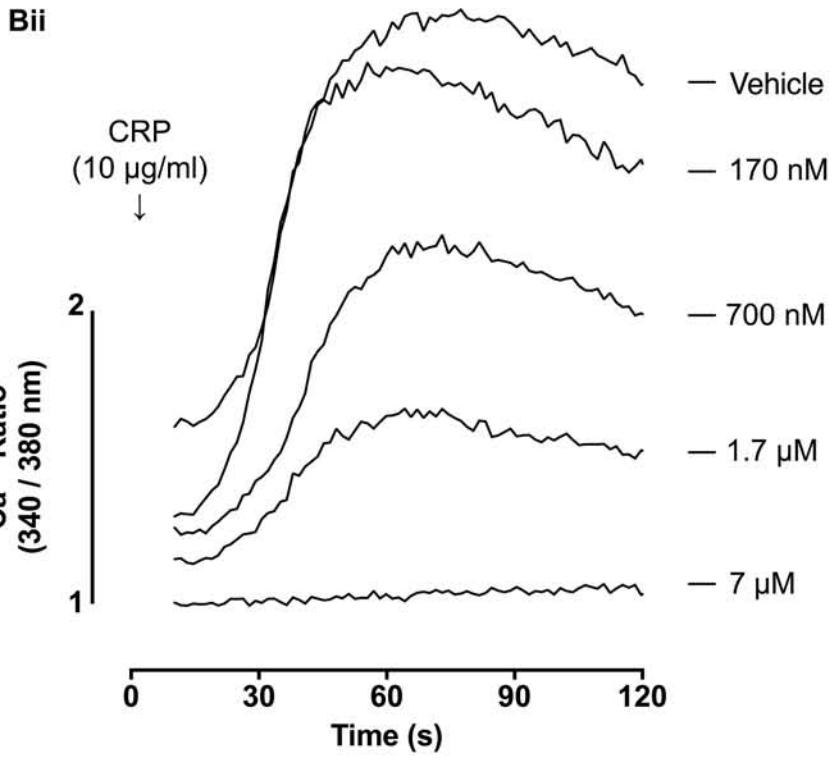
Bii
Vehicle
CRP
(10 µg/ml)
170 nM
700 nM
2
1
Ca2+ Ratio
(340 / 380 nm)
1.7 µM
7 µM
0
30
60
90
120
Time (s)

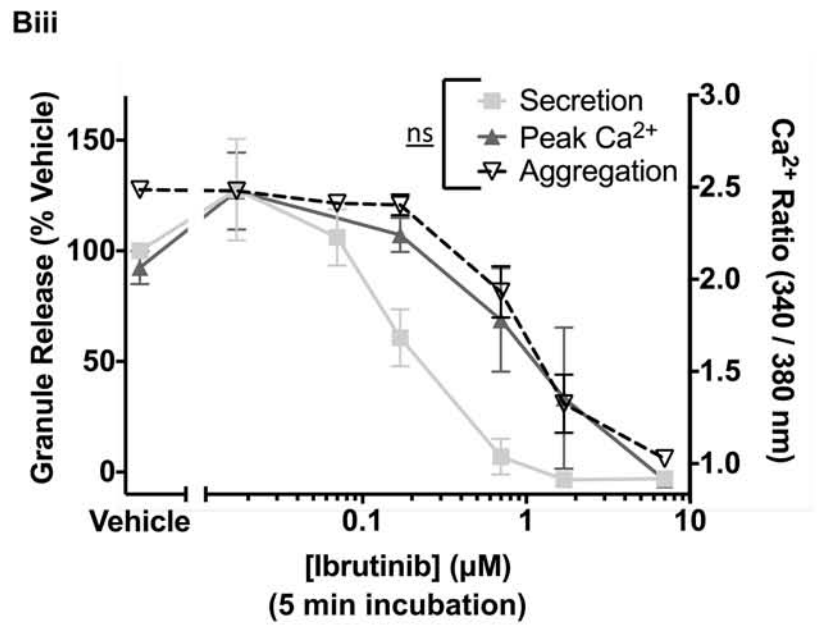
Biii
Secretion
ns
Peak Ca2+
Aggregation
150
100
50
0
Granule Release (% Vehicle)
3.0
2.5
2.0
1.5
1.0
Ca2+ Ratio (340 / 380 nm)
Vehicle
0.1
1
10
[Ibrutinib] (µM)
(5 min incubation)

Figure 3

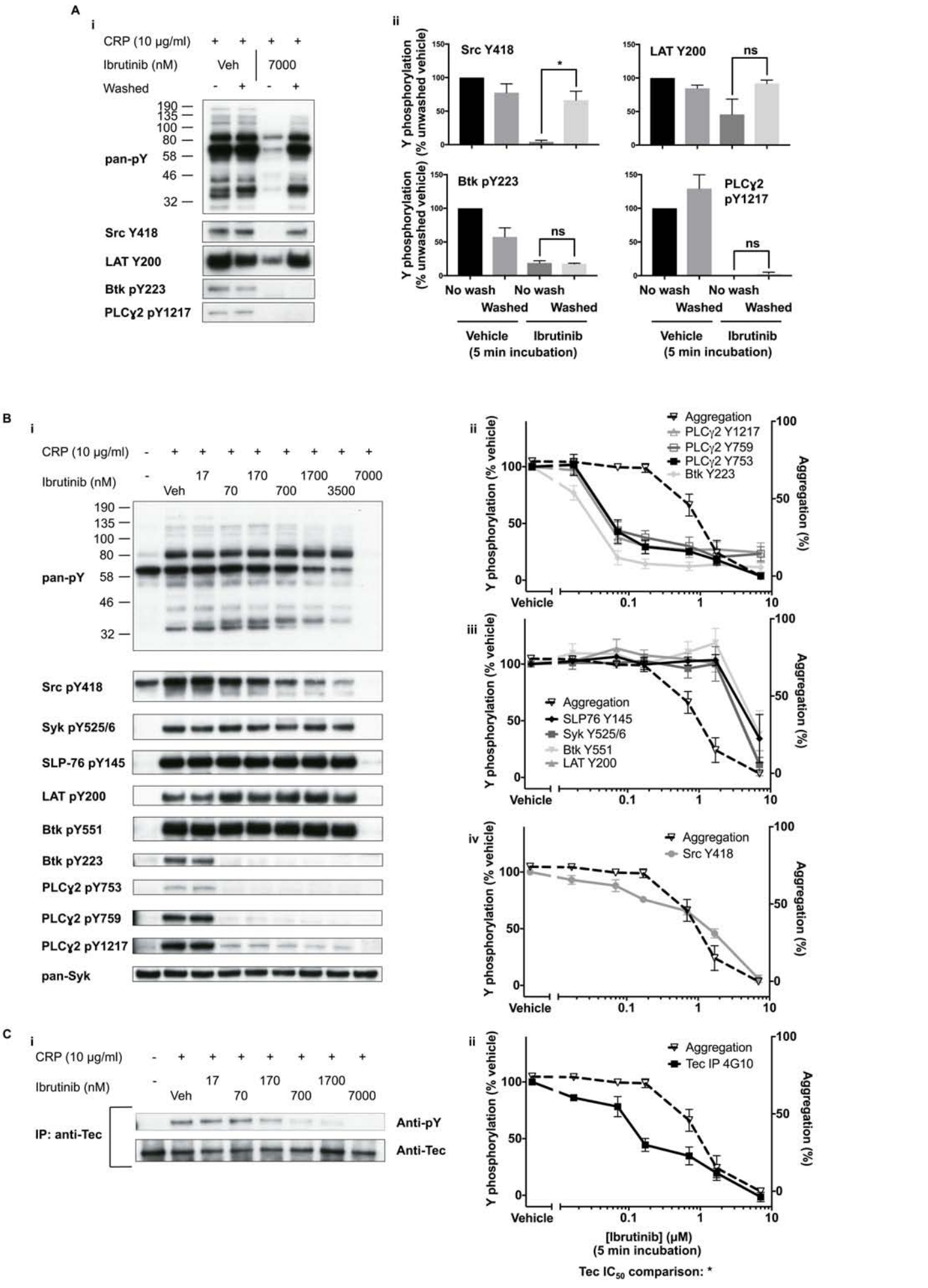
A
i
CRP (10 µg/ml) + + + +
Ibrutinib (nM) Veh 7000
Washed - + - +
190
135
100
80
pan-pY 58
46
32
Src Y418
LAT Y200
Btk pY223
PLCγ2 pY1217
ii
Y phosphorylation (% unwashed vehicle)
Src Y418
*
LAT Y200
ns
Btk pY223
ns
PLCγ2 pY1217
ns
No wash
Washed
No wash
Washed
Vehicle
Ibrutinib
(5 min incubation)
B
i
CRP (10 µg/ml) - + + + + + + + +
Ibrutinib (nM) - 17 170 1700 7000
Veh 70 700 3500
pan-pY
Src pY418
Syk pY525/6
SLP-76 pY145
LAT pY200
Btk pY551
Btk pY223
PLCγ2 pY753
PLCγ2 pY759
PLCγ2 pY1217
pan-Syk
ii
Aggregation
PLCγ2 Y1217
PLCγ2 Y759
PLCγ2 Y753
Btk Y223
Y phosphorylation (% vehicle)
Aggregation (%)
Vehicle
iii
Aggregation
SLP76 Y145
Syk Y525/6
Btk Y551
LAT Y200
iv
Aggregation
Src Y418
C
i
CRP (10 µg/ml) - + + + + + + +
Ibrutinib (nM) - 17 170 1700
Veh 70 700 7000
IP: anti-Tec
Anti-pY
Anti-Tec
ii
Aggregation
Tec IP 4G10
[Ibrutinib] (µM)
(5 min incubation)
Tec IC50 comparison: *

Figure 4

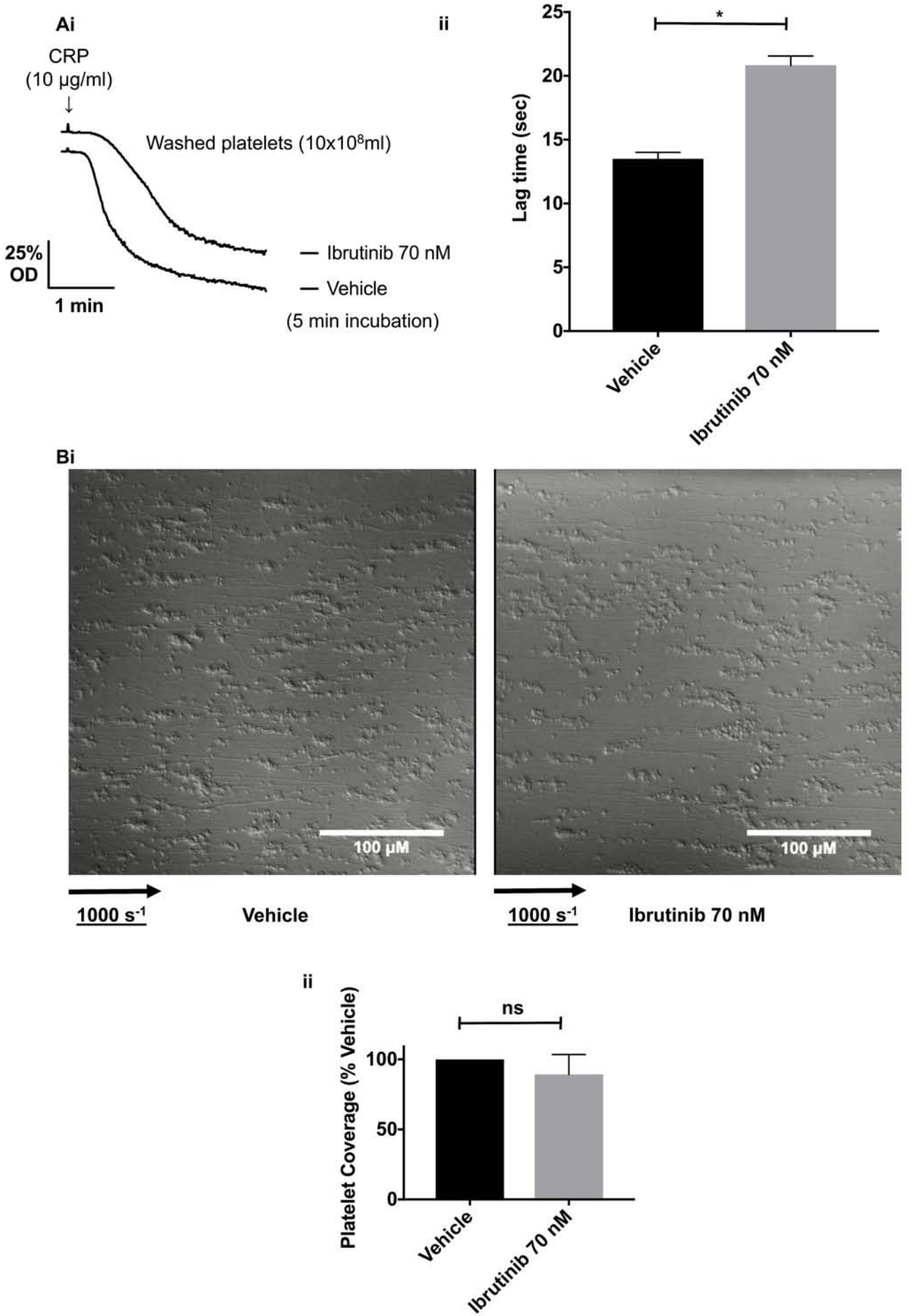
Ai
CRP
(10 µg/ml)
Washed platelets (10x10⁸ml)
25%
OD
1 min
— Ibrutinib 70 nM
— Vehicle
(5 min incubation)
ii
Lag time (sec)
25
20
15
10
5
0
*
Vehicle
Ibrutinib 70 nM
Bi
100 µM
100 µM
1000 s⁻¹
Vehicle
1000 s⁻¹
Ibrutinib 70 nM
ii
Platelet Coverage (% Vehicle)
100
50
0
ns
Vehicle
Ibrutinib 70 nM

Figure 5

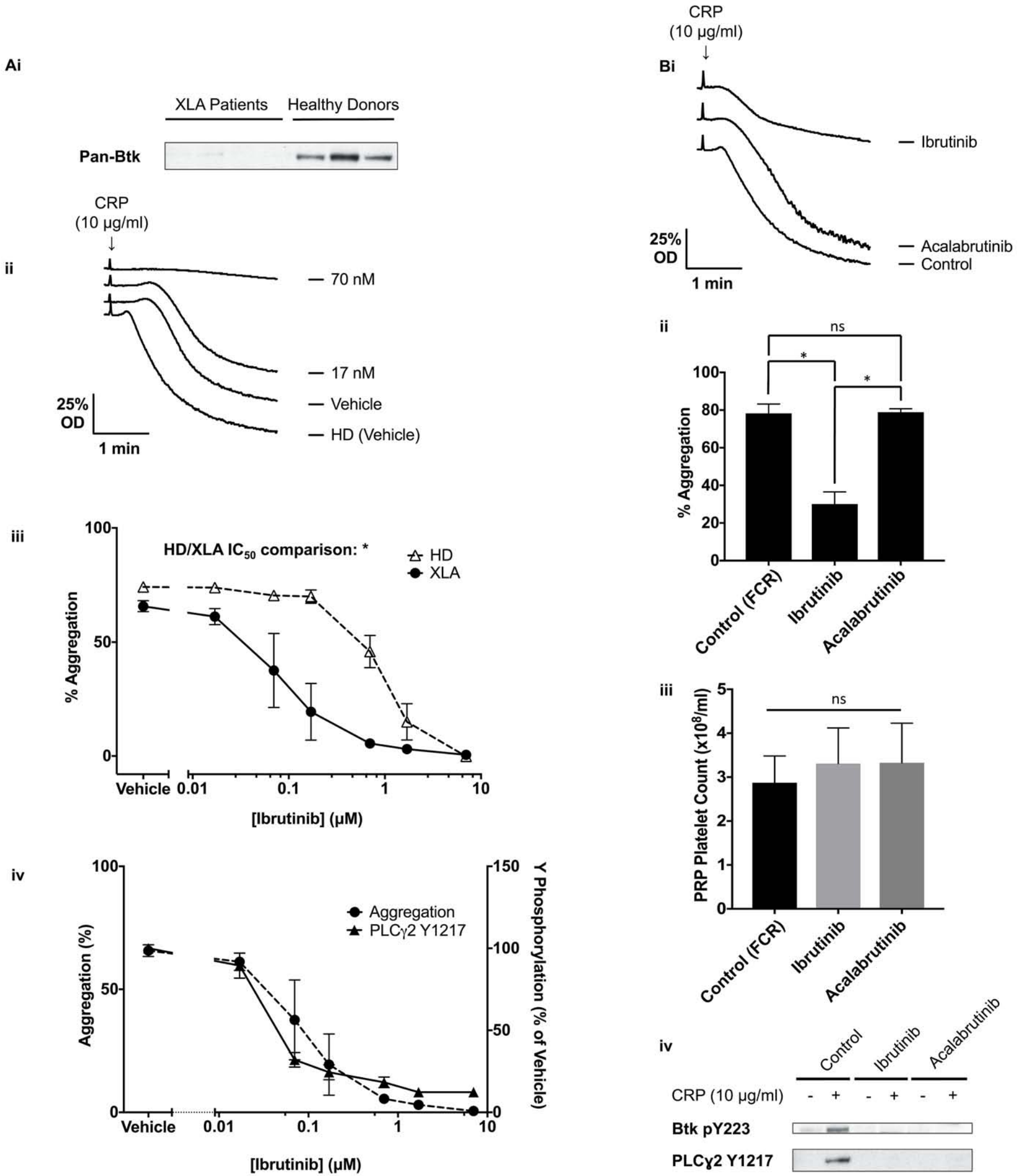
Ai
XLA Patients
Healthy Donors
Pan-Btk
ii
CRP
(10 µg/ml)
70 nM
17 nM
Vehicle
HD (Vehicle)
25%
OD
1 min
iii
HD/XLA IC50 comparison: *
HD
XLA
% Aggregation
Vehicle
0.01
0.1
1
10
[Ibrutinib] (µM)
iv
Aggregation
PLCγ2 Y1217
Aggregation (%)
Y Phosphorylation (% of Vehicle)
Vehicle
0.01
0.1
1
10
[Ibrutinib] (µM)
Bi
CRP
(10 µg/ml)
Ibrutinib
Acalabrutinib
Control
25%
OD
1 min
ii
ns
*
*
% Aggregation
Control (FCR)
Ibrutinib
Acalabrutinib
iii
ns
PRP Platelet Count (x10^8/ml)
Control (FCR)
Ibrutinib
Acalabrutinib
iv
Control
Ibrutinib
Acalabrutinib
CRP (10 µg/ml)
- + - + - +
Btk pY223
PLCγ2 Y1217

Figure 6

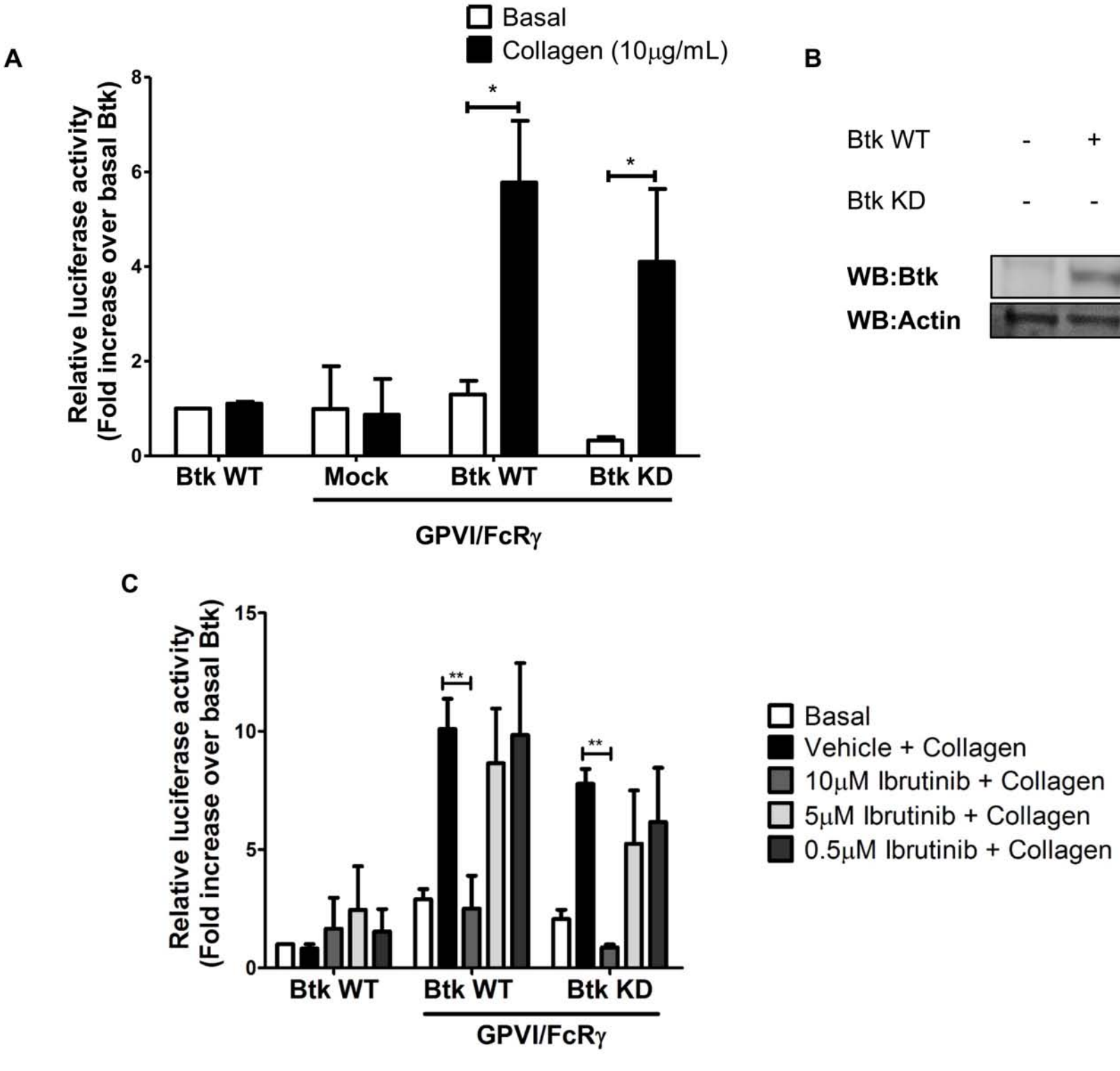
A
Basal
Collagen (10μg/mL)
Relative luciferase activity
(Fold increase over basal Btk)
8
6
4
2
0
*
*
Btk WT
Mock
Btk WT
Btk KD
GPVI/FcRγ
B
Btk WT - + -
Btk KD - - +
WB:Btk
WB:Actin
C
Relative luciferase activity
(Fold increase over basal Btk)
15
10
5
0
**
**
Btk WT
Btk WT
Btk KD
GPVI/FcRγ
Basal
Vehicle + Collagen
10μM Ibrutinib + Collagen
5μM Ibrutinib + Collagen
0.5μM Ibrutinib + Collagen

Figure 7

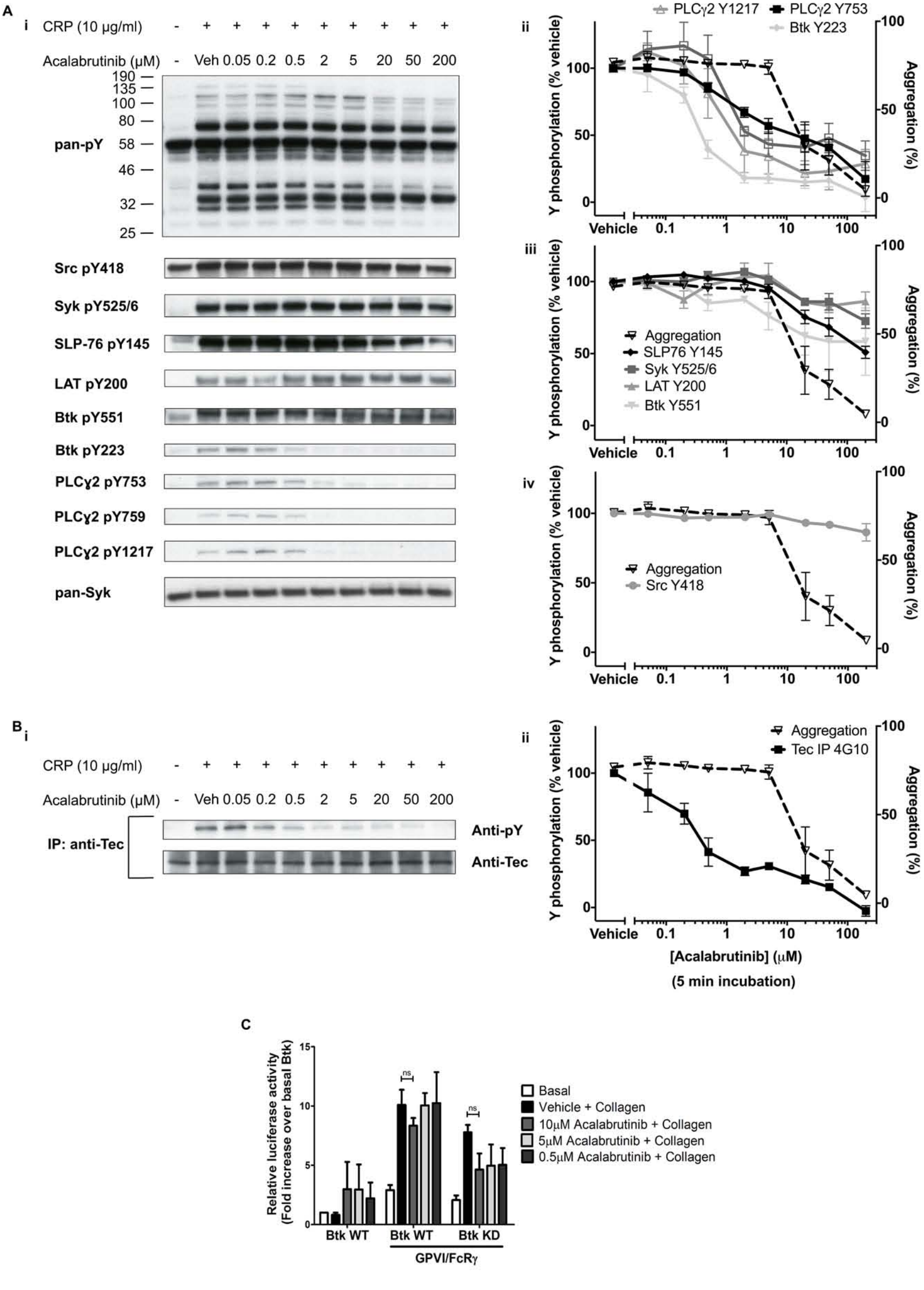
A
i
CRP (10 µg/ml) - + + + + + + + + +
Acalabrutinib (µM) - Veh 0.05 0.2 0.5 2 5 20 50 200
190
135
100
80
pan-pY 58
46
32
25
Src pY418
Syk pY525/6
SLP-76 pY145
LAT pY200
Btk pY551
Btk pY223
PLCγ2 pY753
PLCγ2 pY759
PLCγ2 pY1217
pan-Syk
ii
Aggregation
PLCγ2 Y759
PLCγ2 Y1217
PLCγ2 Y753
Btk Y223
Y phosphorylation (% vehicle)
Aggregation (%)
Vehicle 0.1 1 10 100
iii
Aggregation
SLP76 Y145
Syk Y525/6
LAT Y200
Btk Y551
iv
Aggregation
Src Y418
B
i
CRP (10 µg/ml) - + + + + + + + + +
Acalabrutinib (µM) - Veh 0.05 0.2 0.5 2 5 20 50 200
IP: anti-Tec
Anti-pY
Anti-Tec
ii
Aggregation
Tec IP 4G10
Y phosphorylation (% vehicle)
Aggregation (%)
Vehicle 0.1 1 10 100
[Acalabrutinib] (µM)
(5 min incubation)
C
Relative luciferase activity (Fold increase over basal Btk)
ns
Basal
Vehicle + Collagen
10µM Acalabrutinib + Collagen
5µM Acalabrutinib + Collagen
0.5µM Acalabrutinib + Collagen
Btk WT
Btk WT
Btk KD
GPVI/FcRγ

Supplementary Data

Methods

Reagents

The α-phosphotyrosine (4G10) monoclonal antibody (mAb) was from Millipore (Abingdon, UK). The α-Syk pAb (SC-1077) was from Santa Cruz Biotechnology (Dallas, USA). The α-Btk pAb (SAB3500372) was from Sigma-Aldrich (Poole, UK). Phosphospecific pAbs against Syk pY525/6, PLCɣ2 pY759 and pY1217, were from Cell Signalling Technology (Hitchin, UK) and against LAT pY200, SLP-76 PY145, PLCɣ2 Y753, Btk pY223 and pY551 were from Abcam (Cambridge, UK). Ibrutinib (PCI-32765) and acalabrutinib (ACP-196) were from Selleckchem (Munich, Germany). Eptifibatide was from GSK (Brentford, UK). The α-Tec and α-Btk pAbs (BL17 and BL19 respectively) have been described[22]. HRP-conjugated secondary pAbs and Hyperfilm ECL autoradiography film were from Amersham Biosciences (GE Healthcare, Bucks, UK). ECL reagent and the Ca^{2+} sensitive report precursor dye Fura-2-AM were from ThermoFisher (Waltham, MA). CRP was from Richard Farndale (Cambridge, UK). Collagen was made from equine tendon and sourced from Takeda (Linz, Austria). ChronoLume® and ATP standard were from ChronoLog Corporation (Havertown, PA). All other reagents were purchased from Sigma-Aldrich (Poole, UK).

Chemical analysis of inhibitors

Purity assessment of individual batches of ibrutinib and acalabrutinib was performed by High Performance Liquid Chromatography and Liquid Chromatograpy Mass Spectrometry. Individual batches of inhibitor were compared to each other using lumiaggregometry to CRP in washed platelets as a bioassay. Concentration calculations for each batch of inhibitor were adjusted to reflect their differences in potency in this bioassay when compared to the measured chemical concentration.

Platelet rich plasma (PRP) and washed platelet preparation

Blood was taken from consenting patients or healthy, drug-free volunteers, into 4% sodium citrate. Blood from patients, who were not taking concomitant antiplatelet medication, was taken at 2-3 hours after the ingestion of Btk inhibitor on the final day of a treatment cycle. PRP was obtained by centrifugation at 200 *g* for 20 min at room temperature. Washed platelets were obtained by centrifugation at 1,000 *g* for 10 min using 0.2 μg/mL prostacyclin and resuspended in modified-Tyrode's-HEPES buffer (134 mM NaCl, 0.34 mM Na_2HPO_4, 2.9 mM KCl, 12 mM $NaHCO_3$, 20 mM HEPES, 5 mM glucose, 1 mM $MgCl_2$; pH 7.3) as previously described[39]. Platelets were used at 4×10^8/mL for aggregation and biochemistry unless otherwise stated.

Granule Release

During LTA, 5 μL ChronoLume® (a commercial reagent containing a D-luciferin-luciferase mixture) was added 1 min prior to insertion of glass vials into the

measurement chamber of the aggregometer. Light production by luciferase was measured by the Model 700 aggregometer. Calibration was performed by adding 5 µL of 2 µM ATP standard at the end of the experiment. Results were averaged and IC_{50} values were calculated from these data.

Measurement of $[Ca^{2+}]_i$

Platelets were loaded with the Ca^{2+} sensitive dye Fura-2 by incubation of PRP with 2 µM Fura-2-AM for 1 hour at 30°C. Platelets were then washed by centrifugation at 350 *g* for 20 min and resuspended in modified-Tyrode-HEPES buffer. Fura-2-loaded platelets were incubated with inhibitors or vehicle (DMSO) for 5 min at 37°C prior to addition of agonists. Fluorescence measurements with excitation at 340 and 380 nm and emission at 510 nm were recorded over a period of 5 min using a NOVOstar plate reader (BMG Labtech) for experiments with ibrutinib or a FlexStation (Molecular Devices) for experiments with acalabrutinib. $[Ca^{2+}]_i$ was calculated using the ratio of the 340 and 380 nm excitation signals according to the method of Grynkiewicz *et al*[40]. Results were averaged and IC_{50} values were calculated from these data.

Measurement of platelet adhesion under flow

Washed platelets were incubated with inhibitor or vehicle for 5 min. Platelets were added back to non-ACD treated red blood cells and Platelet Poor Plasma (PPP) to a final concentration of $4x10^8$/mL. Platelets were incubated with 4 µM $DiOC_6$ for 5 min to aid visualisation. Flow adhesion using a Cellix microfluidic system was performed as described[13]. Microcapillaries were subsequently fixed with 10% neutral buffered Formalin solution and platelet adhesion was viewed using a Zeiss Axio Observer 7 microscope at 20X objective using fluorescence intensity emitted at 520 nm. Platelet surface coverage on flow adhesion microcapillary images were measured using ImageJ 1.5.

Cells and plasmids

The DT40 chicken lymphoma cell line rendered deficient in Btk[41] was cultured in RPMI 1640 medium supplemented with 10% fetal bovine serum, 1% chicken serum, 100 U/ml penicillin, 100 µg/mL streptomycin, 20 mM glutamine and 50 µM 2β-mercaptoethanol. GPVI, FcRɣ and NFAT-luciferase plasmids have been described previously[42]. The WT and K430E Btk plasmids have been previously described[26].

Transfections and luciferase assay

Cells were transfected in a volume of 0.4 mL of serum free RPMI using a Gene Pulser II Electroporator (Bio-Rad) set at 350 V and 500 µF. Cells were transfected with 2 µg of both GPVI and FcRɣ, and 7.5 µg of NFAT-luciferase plasmids and where stated, either 5 µg WT or KD Btk plasmids. Twenty hours after transfection, live cells were counted by Trypan blue exclusion and diluted to $2x10^6$/mL. Cells (50 µL) were stimulated with 50 µL Horm collagen (10 µg/mL final concentration) (Nycomed, Germany) for 6 hours. In experiments involving ibrutinib and acalabrutinib, cells were

stimulated with collagen (10 µg/mL final) in the presence of ibrutinib (0.5-10 µM), acalabrutinib (0.5-10 µM) or vehicle (0.2% DMSO) for 6 hours in the absence of serum as these drugs have a high degree of plasma binding{Honigberg:2010hh}. Cells were then lysed with 11 µL of lysis buffer (10% Triton X-100, 200 mM $NaPO_4$ (pH 7.8), and 4 mM dithiothreitol) and added to an equal volume of assay buffer (200 mM $NaPO_4$, 20 mM $MgCl_2$ and 10 mM ATP). Luciferase activity was measured using a NOVOstar plate reader (BMGLabtech) following the addition of 50 µL of 1 mM D-luciferin. Luciferase assay values were recorded in triplicate and averaged. The luciferase assay data were normalized to basal wild-type Btk values.

Figures

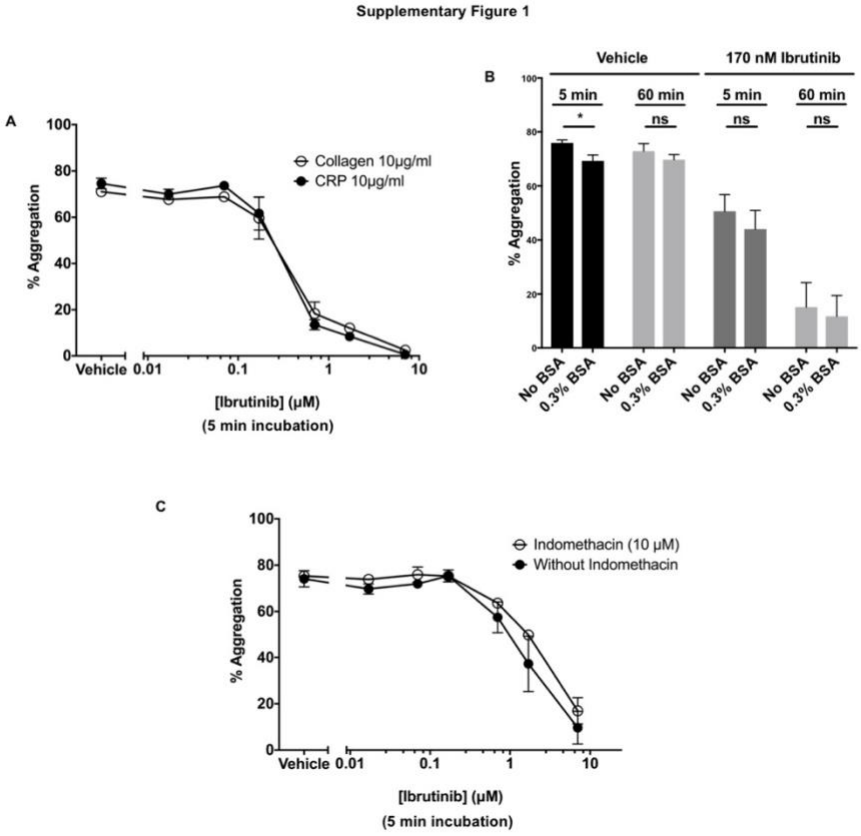
Supplementary Figure 1
A
% Aggregation
Collagen 10µg/ml
CRP 10µg/ml
Vehicle
0.01
0.1
1
10
[Ibrutinib] (µM)
(5 min incubation)
B
Vehicle
170 nM Ibrutinib
5 min
60 min
5 min
60 min
*
ns
ns
ns
% Aggregation
No BSA
0.3% BSA
C
Indomethacin (10 µM)
Without Indomethacin
% Aggregation
[Ibrutinib] (µM)
(5 min incubation)

Supplementary Figure 2

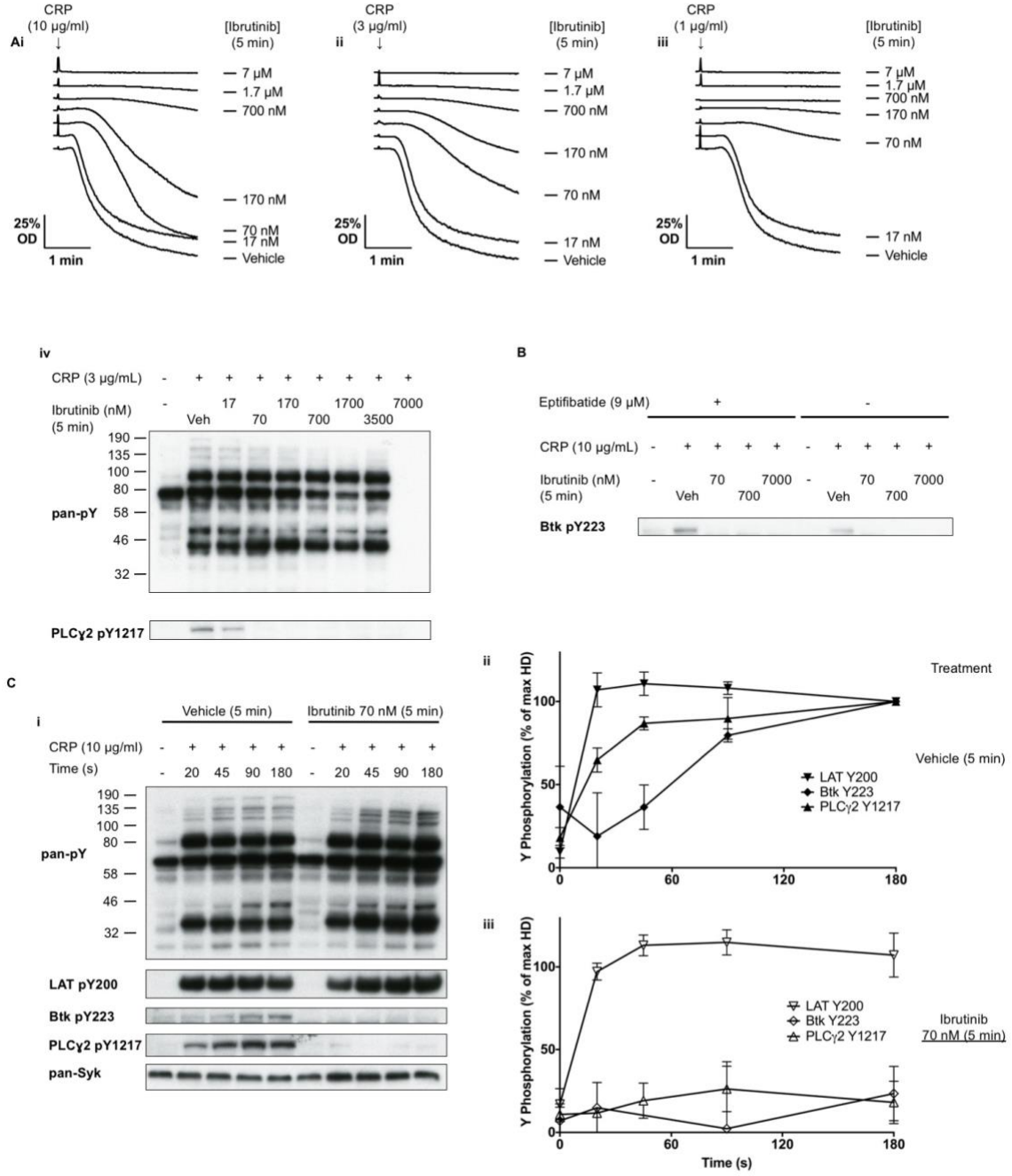

Supplementary Figure 3

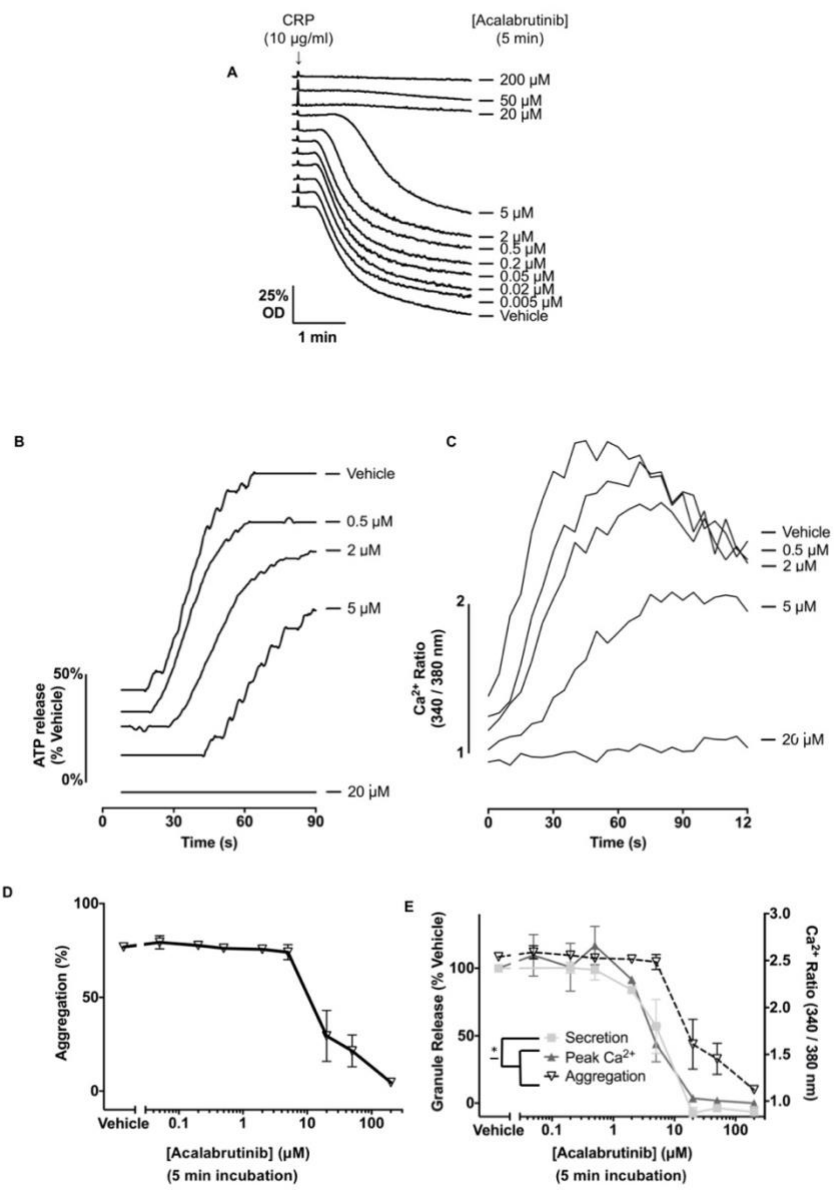

Supplementary Table 1. IC_{50} values for dose response curves (all numbers in μM)

Ibrutinib containing figures	**Name of Curve**	**IC_{50} (μM)**	**95% C.I.**
2Aiii	HD Aggregation	1.19	0.73 – 1.95
2B	HD Secretion	0.25	0.121 – 0.548
2B	HD Ca^{2+} Mobilisation	1.88	0.445 – 22.18
3Aii	HD Btk pY223	0.023	0.014 – 0.036
3Aii	HD PLCɣ2 pY1217	0.035	0.019 – 0.065
3Aii	HD PLCɣ2 pY759	0.048	0.026 – 0.088
3Aii	HD PLCɣ2 pY753	0.055	0.029 – 0.105
3Aiii	HD Syk pY525/6	-	-
3Aiii	HD LAT pY200	-	-
3Aiii	HD SLP-76 pY145	-	-
3Aiii	HD Btk pY551	-	-
3Aiv	HD Src pY418	2.1	1.24 – 3.7
5Aiii	XLA Aggregation	0.086	0.037 – 0.212
5Aiv	XLA PLCɣ2 pY1217	0.035	0.014 – 0.087
Acalabrutinib containing figures			
7Aii	HD Btk pY223	0.308	0.177 – 0.549
7Aii	HD PLCɣ2 pY1217	0.88	0.393 – 2.07
7Aii	HD PLCɣ2 pY759	1.211	0.479 – 3.244
7Aii	HD PLCɣ2 pY753	2.75	1.20 – 6.59
7Aiii	HD Syk pY525/6	-	-
7Aiii	HD LAT pY200	-	-
7Aiii	HD SLP-76 pY145	-	-
7Aiii	HD Btk pY551	-	-
7Aiv	HD Src pY418	-	-
Supp Fig 3D	HD Aggregation	21.25	12.27 – 37.11
Supp Fig 3E	HD Secretion	6.37	3.706 – 11.02
Supp Fig 3E	HD Ca^{2+} Mobilisation	5.317	2.843 – 10.15

Supplementary Table 2. Btk mutations of XLA patients

Patient	Mutation	Predicted effect
1	c. 1750+1G>A	5′ donor site of exon 17 abolished
2	c. 700C>T	Stop codon at Gln234
3	c. 710del	Frameshift with premature termination
4	c. 1820C>A	Mutation likely to affect the kinase domain

Figure Legends

Supplementary Figure 1. Ibrutinib dose dependently inhibits GPVI-mediated aggregation, ATP secretion and Ca^{2+}.
(A) Healthy donor washed platelets ($4x10^8$/mL) we incubated with ibrutinib or vehicle (DMSO) at the stated doses for 5 min. These were then stimulated with CRP (10 µg/mL) or collagen (10 µg/mL) for 180 sec. (B) Washed platelets in the presence or absence of 0.3% BSA were incubated with ibrutinib or vehicle (DMSO) at the stated doses in the for the stated time before being stimulated with CRP (10 µg/mL). Results shown are representative of three independent experiments. * $p < 0.05$, ns = not significant. (C) Healthy donor washed platelets ($4x10^8$/mL) we incubated with ibrutinib or vehicle (DMSO) at the stated doses for 5 min in the presence or absence of 10 µM indomethacin. These were then stimulated with CRP (10 µg/mL) for 180 sec. Data shown are mean ± SEM of three identical experiments.

Supplementary Figure 2. Reducing the concentration of the CRP or the presence or absence of eptifibatide does not change the dose range over which ibrutinib has its effects or the concentration at which it blocks tyrosine phosphorylation at and downstream of Btk. (A) Healthy donor washed platelets ($4x10^8$/mL) were incubated with ibrutinib or vehicle (DMSO) at the stated doses for 5 min. Representative traces of stimulation with CRP at (i) 10 µg/mL, (ii) 3 µg/mL or (iii) 1 µg/mL for 180 sec are shown. Washed platelets ($4×10^8$/mL) were stimulated for 180 sec with (iv) CRP (3 µg/mL) in the presence of eptifibatide (9 µM) or (B) CRP (10 µg/mL) in the presence or absence of eptifibatide (9 µM) followed by lysis with 5X SDS reducing sample buffer. Prior to addition of agonist, platelets were pre-incubated with either ibrutinib or vehicle (DMSO) for 5 min. Whole cell lysates were then separated by SDS-PAGE and Western blot with the stated antibodies for whole cell phosphorylation and kinases downstream of GPVI. (C) Whole cell lysates were made at the time points shown after stimulation with CRP (10 µg/ml) in the presence or absence of low dose (70 nM) ibrutinib incubated for 5 min. These were then separated by SDS-PAGE and western blot was performed with the stated antibodies. Representative blot (i), quantification of band intensity relative to healthy donor at 180 sec without (ii) and with (iii) low dose ibrutinib (n=3). Aggregation traces and blots are representative of three similar experiments.

Supplementary Figure 3. Acalabrutinib dose dependently inhibits GPVI-mediated platelet aggregation, ATP secretion and Ca^{2+} mobilisation. (A) Representative traces showing effect of increasing doses of *in vitro* acalabrutinib incubated for 5 min in washed platelets for (A) aggregometry, (B) ATP secretion and (C) and Ca^{2+} mobilisation. (D) Acalabrutinib dose response curve for aggregation in washed platelets (n=3). (E) Acalabrutinib dose response curves in washed platelets with ATP secretion (n=3) and Ca^{2+} mobilisation (n=3). The dose response curve for inhibition of washed platelet aggregation from (D) is shown as a dotted line to enable comparison. Results are shown as mean ± SEM. All experiments were stimulated with CRP (10 µg/mL).